ornl

OAK RIDGE NATIONAL LABORATORY

UNION CARBIDE

MASTER

Summary of ENDF/B-V Evaluations for Carbon, Calcium, Iron, Copper, and Lead and ENDF/B-V Revision 2 for Calcium and Iron

C. Y. Fu

OPERATED BY
UNION CARBIDE CORPORATION
FOR THE UNITED STATES
DEPARTMENT OF ENERGY

DISCLAIMER

This report was prepared as an account of work sponsored by an agency of the United States Government. Neither the United States Government nor any agency Thereof, nor any of their employees, makes any warranty, express or implied, or assumes any legal liability or responsibility for the accuracy, completeness, or usefulness of any information, apparatus, product, or process disclosed, or represents that its use would not infringe privately owned rights. Reference herein to any specific commercial product, process, or service by trade name, trademark, manufacturer, or otherwise does not necessarily constitute or imply its endorsement, recommendation, or favoring by the United States Government or any agency thereof. The views and opinions of authors expressed herein do not necessarily state or reflect those of the United States Government or any agency thereof.

DISCLAIMER

Portions of this document may be illegible in electronic image products. Images are produced from the best available original document.

Engineering Physics Division

SUMMARY OF ENDF/B-V EVALUATIONS FOR CARBON, CALCIUM, IRON, COPPER, AND LEAD AND ENDF/B-V REVISION 2 FOR CALCIUM AND IRON

C. Y. Fu

NOTICE This document contains information of a preliminary nature. It is subject to revision or correction and therefore does not represent a final report.

THIS PAGE

WAS INTENTIONALLY

LEFT BLANK

CONTENTS

SUMMARY OF ENDF/B-V EVALUATIONS FOR CARBON, CALCIUM, IRON, COPPER, AND LEAD AND ENDF/B-V REVISION 2 FOR CALCIUM AND IRON

C. Y. Fu

ABSTRACT

This report, together with documents already published, describes the ENDF/B-V evaluations of the neutron and gamma-ray-production cross sections for carbon, calcium, iron, copper, and lead and the ENDF/B-V Revision 2 evaluations for calcium and iron.

1. INTRODUCTION

The evaluations of the neutron and gamma-ray-production cross sections for calcium, iron, and lead began with ENDF/B-III and continued to ENDF/B-V. We were given the responsibility for the carbon evaluation for ENDF/B-IV and the copper evaluation for ENDF/B-V. Further revisions of ENDF/B-V were made in 1981 for calcium and iron. Reports were issued for all the major evaluation efforts. Nuclear model developments and calculations associated with these evaluations have also been published. Minor updates, as well as materials not appropriate for journal articles, are covered in this report. The published works are listed below.

Carbon. The ENDF/B-V evaluation for carbon for incident neutron energies, E_n, less than 4.81 MeV, the threshold of the first excited state of ^{12}C, has been published.[1] The evaluation was aided by R-matrix and variance-covariance analyses. The part for $E_n < 2$ MeV has been adopted as the ENDF/B-V scattering standard[2] for cross-section measurements. The higher energy part of the evaluation is described in Sect. 2.

Calcium. The evaluations for ENDF/B-IV and some major updates for ENDF/B-V were published together.[3] The evaluation was based on a consistent calculation for neutron and gamma-ray-production cross sections with a two-step Hauser-Feshbach model. Some minor updates for ENDF/B-V are covered in Sect. 3. A further revision of ENDF/B-V has already been documented.[4]

Iron. The ENDF/B-V evaluation has been documented.[5,6] Calculational aspects of this evaluation, unchanged since ENDF/B-IV, have also been documented.[7] The calculation was similar to that for calcium but included precompound effects. An evaluation of thermal and resonance capture gamma-ray yields, used since ENDF/B-III, has been separately documented.[8] A further revision of ENDF/B-V (to be released as ENDF/B-V Revision 2 in 1982) is described in Sect. 4.

Copper. Minor updates for ENDF/B-V are described in Sect. 5. Nuclear model calculations for ^{63}Cu which were used to aid the evaluation have been given elsewhere.[9]

Lead. The ENDF/B-III evaluation and part of the ENDF/B-IV evaluation were described in detail[10] and remain mostly valid. The calculational part was repeated for ENDF/B-IV to include precompound effects similar to those used for iron;[7] it has not been documented yet. A summary of ENDF/B-IV and minor updates for ENDF/B-V are described in Sect. 6.

Only the evaluations for the ENDF/B-V general-purpose files are reported here. The evaluations for the ENDF/B-V dosimetry file and activation file will be reported elsewhere.

2. UPDATES FOR CARBON (ENDF/B-V MAT 1306)

Our evaluation for carbon for E_n < 4.81 MeV has been published.[1] The evaluation for E_n > 4.81 MeV is described below.

When work began on carbon for ENDF/B-V, a well-documented French update of ENDF/B-IV had become available.[11] The French evaluation by Lashkar et al.[11] for E_n < 4.81 MeV was taken from ENDF/B-IV and the part for E_n between 4.81 and 8.5 MeV was essentially the same as ENDF/B-IV; however, the part for E_n > 8.5 MeV was substantially improved with newly available data. This was adopted for ENDF/B-V except for the secondary neutron energy distributions from the (n,n'3α) reaction. A covariance file was also added for ENDF/B-V.

2.1 SECONDARY NEUTRON ENERGY DISTRIBUTION FROM THE ^{12}C(n,n'3α) REACTION

Two reasons prompted us to revise the secondary neutron-energy distributions from the (n,n'3α) reaction. First, the distributions given in the French evaluation[11] for E_n > 15 MeV disagree with those inferred from measured alpha-particle energies by Frye et al.[12] For example, for E_n = 20 MeV, the measurement indicates that 70% of the outgoing neutrons are below 5 MeV, while the French evaluation has 10%. In addition, a large portion of secondary neutrons was given in the French evaluation as the continuum (MT91), but it is desirable to represent them as discrete-level excitations so energy-angle kinematics can be accounted for by the existing processing codes.

In the present evaluation, in accordance with Antolkovic and Dolenec,[13] the reaction sequence ^{12}C(n,n')^{12}C(α)^{8}Be(2α) was assumed to account for 90% of the cross section and the sequence ^{12}C(n,α)^{9}Be(n)^{8}Be(2α) account for the remaining 10%. Three other possible reaction sequences had no significant contributions up to 20 MeV.[11,13] A detailed description of the reaction mechanisms and a review of the available literature are given in ref. 11.

A calculation based on the Hauser-Feshbach formalism was used to provide the (n,n') part of the distributions. Ten levels of ^{12}C up to 14 MeV, as given in the French evaluation, were used in the calculation. The spin of the 11.83-MeV level was changed from 2 to 1, according to Antolkovic and Hudomalj.[14] A level density was used for levels above 14 MeV. The density was adjusted to reproduce

the trend[12] in distributions as a function of incident neutron energy. However, the 14-MeV distribution was more strongly influenced by the data of Antolkovic and Delenec.[13] It should be noted that the calculation had little physical basis and was used strictly for extrapolation. The calculation was normalized to 90% of the evaluated cross section for each incident neutron energy and was given in the file as discrete-level excitations.

As for the ^{12}C(n,α) sequence, the French evaluation was followed, and an evaporation spectrum with a temperature of 0.3 MeV was used.

The resulting distribution for 14-MeV incident neutron is shown in Fig. 1. The cross sections for exciting the four lowest levels above the absolute Q-value (7.275 MeV) are given as rectangles with half widths equal to half of the level widths.[11] The cross sections for higher energy levels were lumped with the continuum and given as rectangles with half widths equal to 0.25 MeV. For processing codes that cannot handle level widths, all the cross sections in the ^{12}C(n,n')^{12}C(α)^{8}Be(2α) sequence can be treated as discrete levels. The small evaporation spectrum in Fig. 1 represents the other reaction sequence. To see the spectrum better, the various components were broadened into 0.5-MeV bins and summed as in Fig. 2. This spectrum, if further broadened so that the dip at 10 MeV would almost disappear, would look like the ones experimentally inferred.[12,13] The absolute cross sections for exciting the first few levels are uncertain because they were not clearly resolved experimentally. The mixture of 90% and 10% for the two major reaction sequences may be reasonable at 14 MeV, but not necessarily at other energies. However, the gaps in the spectrum are correctly reproduced.

2.2 COVARIANCE FILE

Covariance data are given for total, elastic, nonelastic, (n,n'), (n,n3α), (n,γ), (n,p), (n,d), and (n,α) cross sections. Derived sections (NC subsections) reflect how the cross-section files were generated.

For total and elastic scattering above 2 MeV, (n,n') and (n,α) cross-section covariances were determined from $\pm 2\sigma$ error bands. The error bands were extended and enlarged to cover energy regions lacking experimental data. In general, long-range covariances reflect systematic errors common to all data sets. Medium-range covariances reflect the difference in energy coverage by different data sets and the difference in the experimental methods within the same data set. Short-range covariances
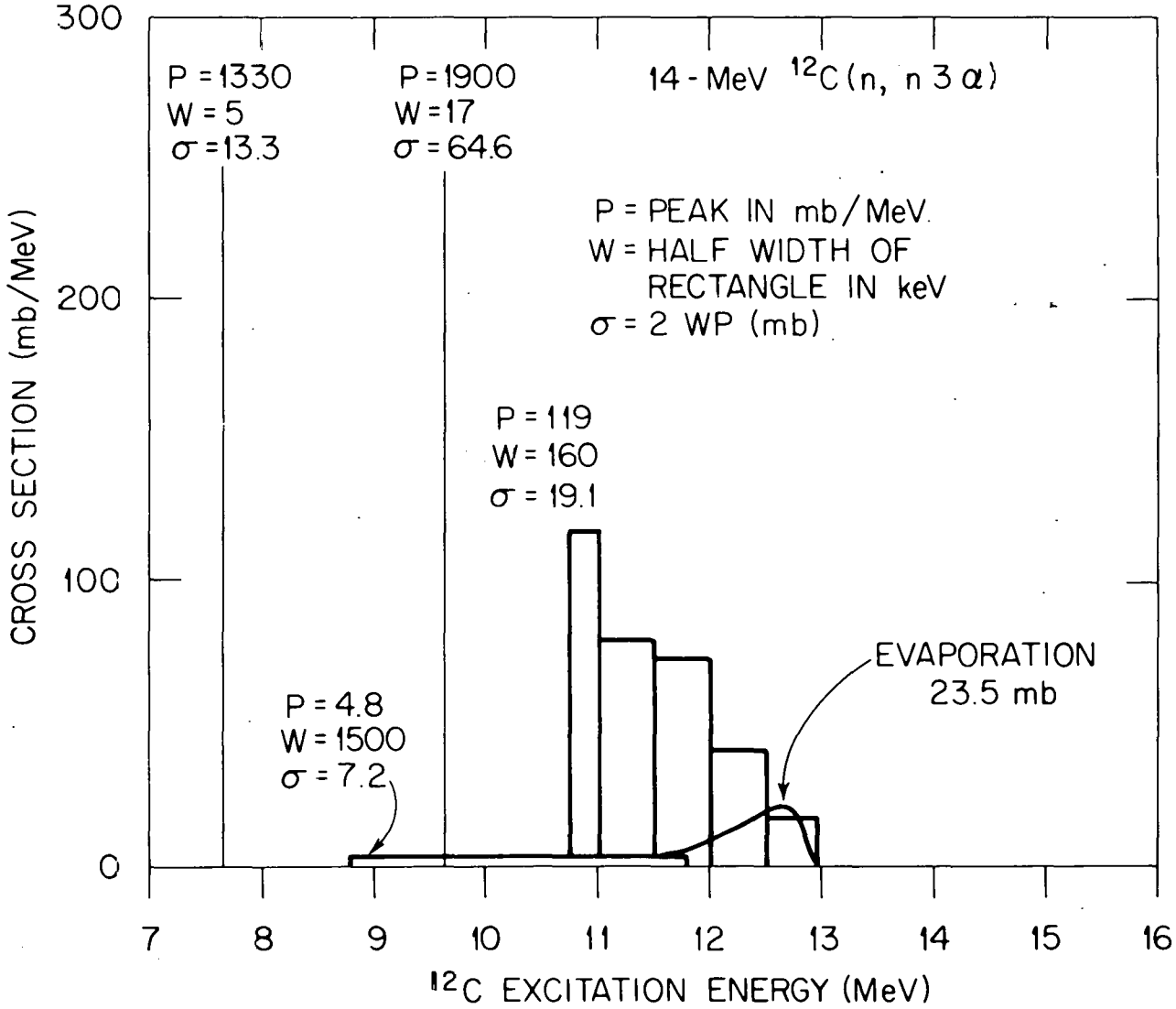
Fig. 1. Excitation cross sections of the discrete levels and continuum bins of ^{12}C in the ^{12}C(n,n'3α) reaction as given in the ENDF/B-V file.

14 - MeV ^{12}C(n, n 3 α)

CROSS SECTION (mb / MeV)

^{12}C EXCITATION ENERGY (MeV)
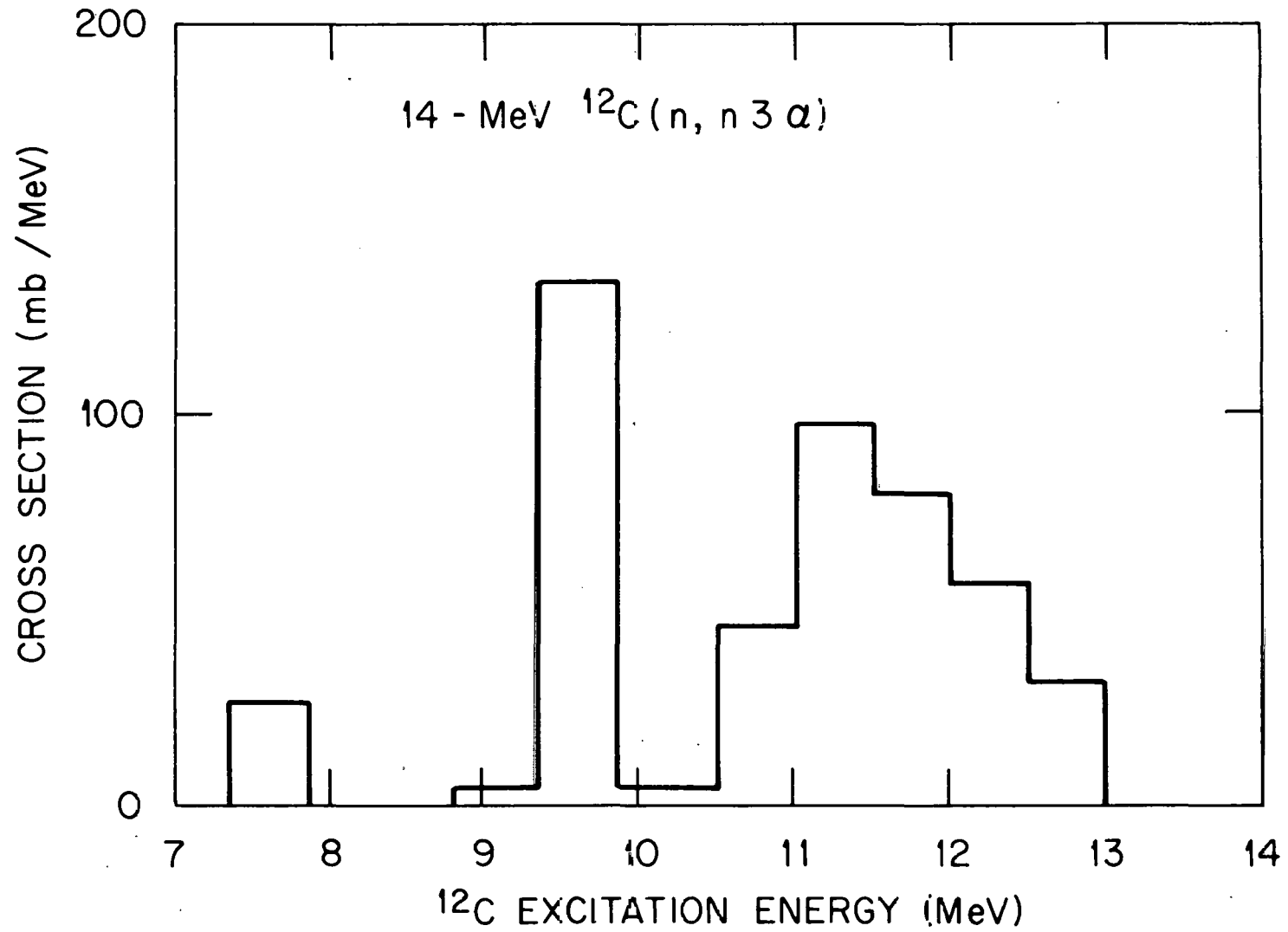
Fig. 2. The spectral components in Fig. 1 are broadened into 0.5-MeV bins and summed.

reflect structures in the cross sections and/or threshold effects. Statistical errors are nonexistent in the evaluated cross sections.

For elastic scattering below 2 MeV, covariances were evaluated individually for each of six data sets. These six data sets and their covariances were averaged by generalized least-squares (Bayes theorem, see ref. 1). The resulting covariances were further modified by considering the effects of the R-matrix fit which included thermal data, data above 2 MeV, and polarization data. Uncertainties (not covariances) in the angular distributions were evaluated and reported in ref. 1. The latter information was not given in the file because covariance formats for angular distributions have not been developed yet.

Seventeen components (either discrete levels or bands of continuum levels) represent the (n,n'3α) reaction cross sections. A 20% fully-correlated uncertainty is given to each component.

3. UPDATES FOR CALCIUM (ENDF/B-V MAT 1320)

The evaluation for ENDF/B-IV and the subsequent revision for ENDF/B-V, except as noted below, have been published together.[3] The ENDF/B-V evaluation was based on a model calculation more advanced than that used for Version IV. For ENDF/B-IV, the reaction cross sections experimentally available below the tertiary reaction threshold (about 8 MeV) were consistently interpreted with the Hauser-Feshbach model with width-fluctuation corrections, but the higher energy part was based on an evaporation model. The latter part of the calculations was repeated for ENDF/B-V following the development of the TNG code[3] which calculates consistently the binary and tertiary reaction cross sections in the Hauser-Feshbach model. It was shown[3] that gamma-ray production spectra from tertiary reactions, such as $^{40}Ca(n,np)$, are sensitive to spin variations and can be reproduced with the new code.

Two minor additional updates for ENDF/B-V are summarized below.

3.1 TOTAL CROSS SECTIONS

Total cross sections from 100 eV to 50 keV were decreased by about 200 mb according to a new high-quality measurement.[15] The new data, some old data, and the ENDF/B-IV values are all graphically shown in BNL-325.[16] The values of the new measurement[15] were chosen for ENDF/B-V.

3.2 CAPTURE CROSS SECTIONS

Capture cross sections from 25 to 200 keV were increased by a factor of 2 to 5 according to recent ORELA data.[17,18] Since resonance parameters are not given in the evaluated files, the cross sections averaged by the experimentalists were used directly as shown in Fig. 3. ENDF/B-IV values are also shown. The cross sections above 200 keV were assumed to decrease, reach a minimum near 5 MeV, increase, and go through a 14-keV value measured by Cvelbar.[19]
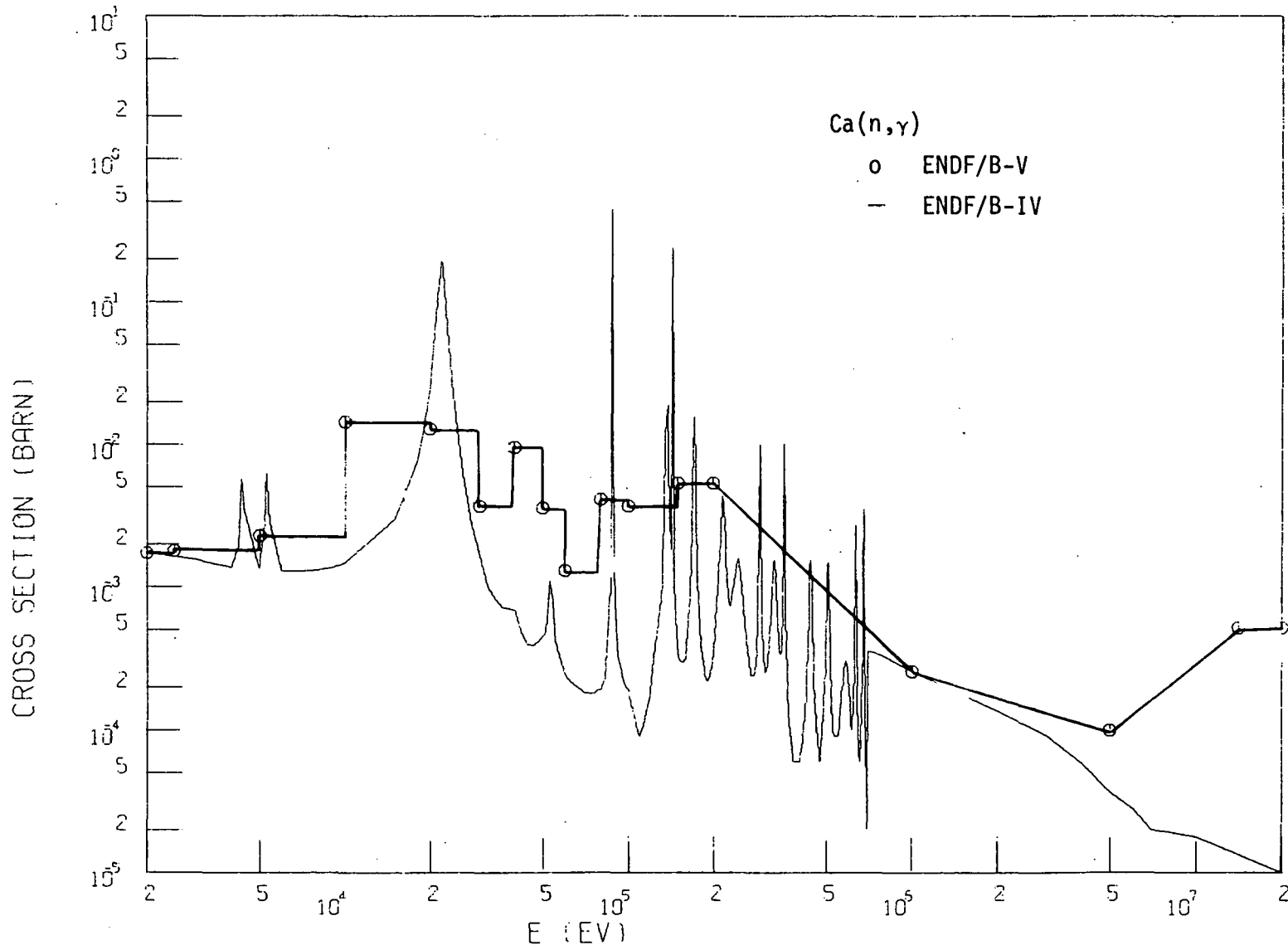
Fig. 3. The Ca(n,γ) cross sections in ENDF/B-IV and -V. The ENDF/B-V values between 2 keV and 200 keV are ORELA data.[17,18]

4. REVISION 2 OF ENDF/B-V MAT 1326 (IRON)

Revisions were made in four areas to the ENDF/B-V evaluation[5,6] for iron and is summarized below. This version will be released in 1982 as ENDF/B-V Revision 2.

4.1 INELASTIC SCATTERING IN ^{57}Fe AND ^{58}Fe

The cross sections for inelastic scattering to 21 levels in ^{57}Fe and two levels in ^{58}Fe were included and combined as 14 sections (MT numbers) as shown in Table 1. Corresponding gamma-ray production data (file 12) and covariance data (file 33) were also provided.

These cross sections were ignored in the ENDF/B-V file for natural iron because of their low abundances: 2.1% for ^{57}Fe and 0.3% for ^{58}Fe. However, for analyses[20,21] of shields or critical assemblies in which iron is the dominant component, the contribution of the low-lying levels of the minor iron isotopes to neutron slowing-down is important. This is mainly because ^{57}Fe is an old isotope whose levels are dense. In particular, its first four existed levels are below 846 keV which is the energy of the first excited state of ^{56}Fe. It is therefore apparent that the low-lying levels of ^{57}Fe cannot be ignored for slowing down of neutrons below 846 keV if there are little or no other materials in the system that have levels comparable in energy to those of ^{57}Fe.

Sensitivity calculations by Kawai et al.[20] for the inelastic scattering cross sections of ^{57}Fe and ^{58}Fe were performed with a central source for a 100-cm-diam iron sphere. It was shown that a neutron flux below 10 keV at 30 cm from a 0.65-MeV source increased 60% after including the cross sections for inelastic scattering to the low-lying levels of ^{57}Fe and ^{58}Fe in the ENDF/B-IV file. Even for a 14-MeV source the increase still amounts to 20%. More recently, an analysis[21] of the Argonne iron benchmark, using the ENDF/B-V iron evaluation, showed that k_{eff} was too low by about 0.7%. After incorporating calculated cross sections for inelastic scattering to the 12 lowest levels of ^{57}Fe into the file, a repeat calculation raised k_{eff} by 0.73%.

For the above reasons, an update for MAT 1326 appeared worthwhile. Since no experimental data were available, the evaluation of the needed cross sections had to be based on model calculations. Level energies, spins, and parities were taken from the *Table of Isotopes*.[22] Optical model parameters were

Table 1. The energy levels of the iron isotopes as grouped for the MT numbers in ENDF/B-V Mod 2

MT (keV)	Fe-54 (keV)	Fe-56 (keV)	Fe-57 (keV)	Fe-58 (keV)
51			14.4	
52			137	
53			367	
54			707	
55				811
56		846		
57			1008	
58			1198,1255,1357	
59	1408			
60			1628,1725	1675
61			1975,1989	
62		2084		
63			2117	
64			2207	
65			2335,2355	
66			2454,2455,2506	
67			2565,2597	
68		2654		
↓		↓		
90		4505		

those found satisfactory for ^{54}Fe and ^{56}Fe by Arthur and Young.[23] Level density parameters were based

on the formalism of Gilbert and Cameron.[24] The TNG1 code[9] was used for the calculation. The code

was based on the Hauser-Feshbach formalism with a consistent treatment of width-fluctuation correc-

tions for the discrete levels and the continuum. A similar calculation for the lowest 12 levels of ^{57}Fe

had been done by Smith.[21] There is a general agreement between the two calculations.

Gamma-ray production cross sections for E_n < 2.122 MeV were based on the branching ratios given

in the *Table of Isotopes*.[22] Some branching ratios were combined, particularly those for the lumped lev-

els. Some weak gamma rays of similar energies were also combined. For E_n > 2.122 MeV, gamma-

ray production data already present in the ENDF/B-V files were based on measurements made for

natural iron, therefore containing the pertinent information for the minor isotopes.

Since all inelastic scattering cross sections for ^{57}Fe and ^{58}Fe were based on calculation, they were

assumed to be fully correlated among the levels and for all energies with an estimated standard devia-

tion of 20%.

4.2 IMPROVED CROSS SECTIONS

The (n,2n), (n,d), (n,t), and (n,^{3}He) cross sections evaluated by Arthur and Young[23] were judged to

be superior to the ENDF/B-V evaluation and were adopted. New data for (n,2n) and (n,d) were used

in their evaluation.[23] The corresponding covariance data in file 33 were slightly adjusted to reflect the

improved knowledge of these cross sections.

4.3 ENERGY BALANCE AND GAMMA-RAY PRODUCTION

Energy imbalances reported by MacFarlane[25] were corrected for E_n between 2.122 and 20 MeV by

adjusting the total gamma-ray production cross sections in file 13 to reproduce the estimated values of

heating per collision. The adjusted results approach those of ENDF/B-IV. The largest changes

occurred for E_n between 12 and 20 MeV. The justification for the adjustment and acceptability of the

results is discussed below.

When evaluating the gamma-ray production cross sections for ENDF/B-IV,[26] there were two major

sets of data available: one by Orphan et al.[27] and one by Dickens et al.[28] using ORELA. Their total

gamma-ray production cross sections for $E_\gamma > 0.68$ MeV are shown in Fig. 4. The two data sets diverge above 5 MeV, differing by as much as a factor of two near 14 MeV. Our calculated results are in good agreement with Orphan et al. below 12 MeV and approach the results of Dickens et al. near 14 MeV. However, our calculated energy distributions agree with Dickens et al. at all energies. Therefore, our calculated total gamma-ray production cross sections were adopted for ENDF/B-IV while using the energy distributions of Dickens et al. The total gamma-ray production cross sections for $E_\gamma > 0.68$ MeV from ENDF/B-IV are shown in Fig. 4.

To resolve the above discrepancy, Chapman et al.[29] undertook a new measurement using ORELA. The raw data were reduced by two methods: pulse height unfolding and pulse height weighting. The former method yielded energy distributions but required good statistics, therefore larger neutron energy bins. Both results are shown in Fig. 4 and agree almost perfectly with those of Orphan et al. To ensure that there were no serious errors in the new measurement, Chapman et al. also made test measurements on carbon, copper, and tantalum which compared with older ORELA results. It was thought that the older measurement by Dickens et al. had some unknown errors and should be superceded by the new measurement. Therefore, we adopted the new measurement for ENDF/B-V.

Recently a consistent calculation of neutron production and gamma-ray production cross sections by Arthur and Young[23] suggested problems in the data of Chapman et al. near 14 MeV. Their calculation at 14 MeV agrees better with ENDF/B-IV than with ENDF/B-V. In addition, the gamma-ray production cross section measured by Drake et al.[14] at an incident neutron energy of 14.2 MeV is closer to that of Dickens et al. than to Chapman et al. At the same time, energy imbalances in the ENDF/B-V iron evaluation were revealed by MacFarlane.[25] Both problems are discussed below.

A detailed calculation was made for the heating per collision using the new evaluated file that has the changes proposed above incorporated into it. The results are shown in Table 2 for some representative energies along with the values derived from our model calculations. The latter values may be good to 20%. The former values are substantially lower than the latter and some are negative, particularly near 14 MeV. It is apparent that the specific energies for either or both the outgoing neutrons and outgoing gamma rays need to be reduced. The specific energy is the energy of the outgoing particle times
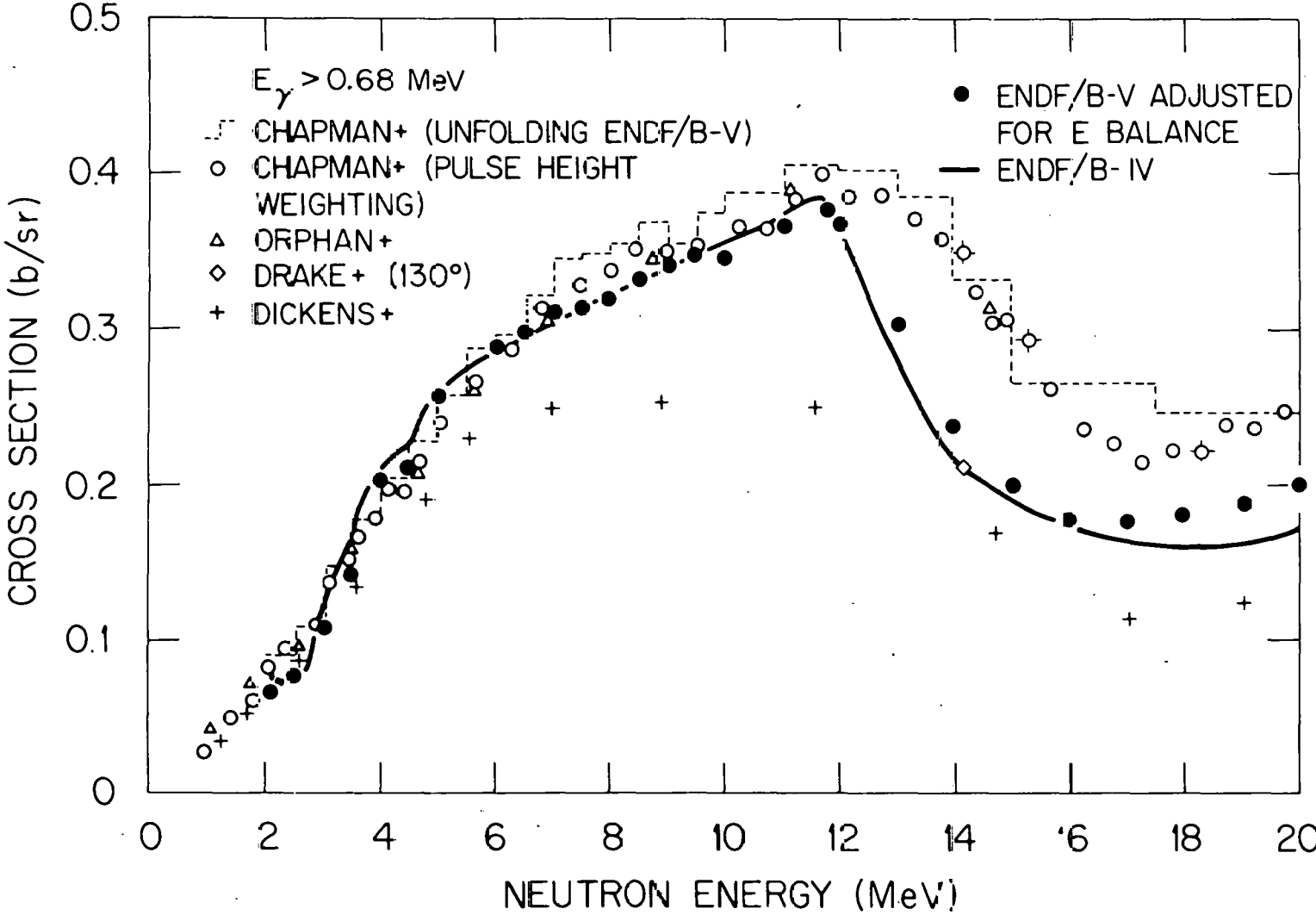
Fig. 4. Various experimental and evaluated gamma-ray production cross sections for natural iron.

Table 2. Some typical heating values calculated from the modified ENDF/B-V (H_5), from model calculations (H_c), and the necessary adjustments in gamma-ray production cross sections

E_n (MeV)	H_5 (MeV)	H_c (MeV)	ΔG_γ (mb)
3	-0.075	0.063	-426
5	0.087	0.117	-76
7	-0.019	0.194	-440
9	0.13	0.301	-280
11	-0.003	0.44	-588
14	-0.463	0.70	-1335
17	0.46	1.03	-1353

its production cross section. Examining all the available data, we found little room for changing either the neutron production cross sections, the secondary neutron energy distributions, or the secondary gamma-ray energy distributions. But as is evident from Fig. 4, there is some flexibility in reducing the gamma-ray production cross sections. Therefore, we adjusted the total gamma-ray-production cross sections to reproduce the more desirable heating values derived from our model calculations. The adjusted results, also shown in Fig. 4 for $E_\gamma > 0.68$ MeV, approach those used in ENDF/B-IV and represent a compromise of all experimental data. The results also agree with the Arthur and Young evaluation.[23]

The total gamma-ray production cross sections in ENDF/B-V was replaced with the adjusted results as a plausible solution to the energy imbalance problem for $E_n > 2.122$ MeV.

For $E_n < 2.122$ MeV, energy imbalances still exist. Here the gamma rays produced are from inelastic scattering and radiative capture. The problem was due to the neutron-energy-dependent capture

gamma-ray spectra given in the file. For each neutron group, the gamma rays produced may be representative of just one isotope, having its own unique Q-value. Therefore, a single Q-value, as required by the ENDF/B-V formats, cannot adequately define the energy balance. This is the well-known "elemental Q-value problem," but solutions other than providing isotopic evaluations are still wanting.

4.4 RESONANCE PARAMETERS

Resonance parameters (file 2) and covariances (file 32) were revised so that the files and the corresponding report[6] are consistent. A few clerical errors were also corrected. However, changes were either very small or involved insignificant resonances.

5. UPDATES FOR COPPER (ENDF/B-V MAT 1329)

Recent high-quality production cross sections of protons and alpha particles near 14 MeV, together with advances in nuclear model codes, have made possible drastic improvement over ENDF/B-IV[31] in these cross sections.[32] The (n,p) cross section near 14 MeV, for example, was reduced by a factor of three. Improvements were also made in some total cross sections and some capture gamma-ray spectra.

5.1 (n,p) AND PROTON PRODUCTION CROSS SECTIONS

The proton production cross section for E_n < 20 MeV in copper is the sum of (n,p), (n,pn), and (n,np) cross sections, or the sum of MT28 and MT103 in terms of the ENDF/B-V formats. Here MT28 represents the sum of the (n,np) and (n,pn) cross sections and, strictly speaking, is incorrectly called the (n,np) cross section.

These cross sections were evaluated separately for each isotope. There was essentially no ^{63}Cu(n,p) measurement for the ENDF/B-IV evaluation. The two data points[32,33] near 14 MeV quoted in BNL-325 (ref. 16) as (n,p) were actually (n,px), thus including a large component for (n,pn). Apparently the ENDF/B-IV evaluators took these values as (n,p) and normalized their calculated curve to the average of these two values. This resulted in an evaluated ^{63}Cu(n,p) cross section at 14 MeV that was a factor of five larger than what was determined below.

Because proton distributions for the two measurements cited above were not available, it was not possible to extract the (n,p) cross section from the (n,px) cross section. Fortunately, a recent Lawrence Livermore National Laboratory (LLNL) measurement by Grimes et al.[34] for the proton production cross section at 14.8 MeV provides detailed proton distributions. These distributions, coupled with advanced model analysis, yielded separate cross sections for the (n,p), (n,pn), and (n,np) reactions as shown in Fig. 5. The details of the calculation (multi-step Hauser-Feshbach with precompound effects) have been documented.[9] The calculated excitation functions shown in Fig. 6 were adopted for ^{63}Cu.

The ^{63}Cu(n,np) cross section at 14 MeV obtained above was 165 mb and was in good agreement with the average of four data points quoted in BNL-325 (ref. 16) which was 170 mb. Note that the (n,np) cross section is meant here instead of the sum of the (n,np) and (n,pn) cross sections.
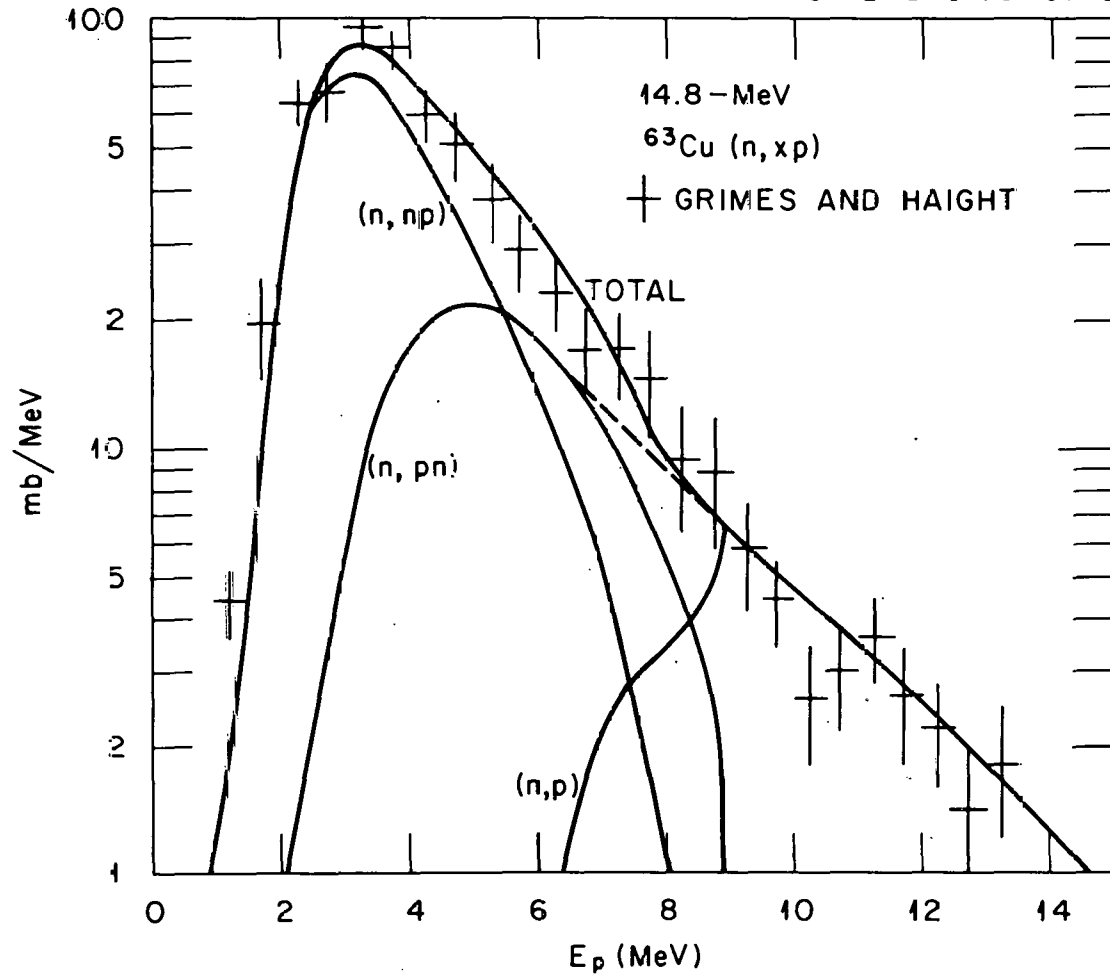
Fig. 5 A model analysis of the measured proton spectrum to extract 14.8-MeV ^{63}Cu(n,p), (n,pn), and (n,np) cross sections. The model code used was TNG,[9] based on multi-particle Hauser-Feshbach and precompound theories.
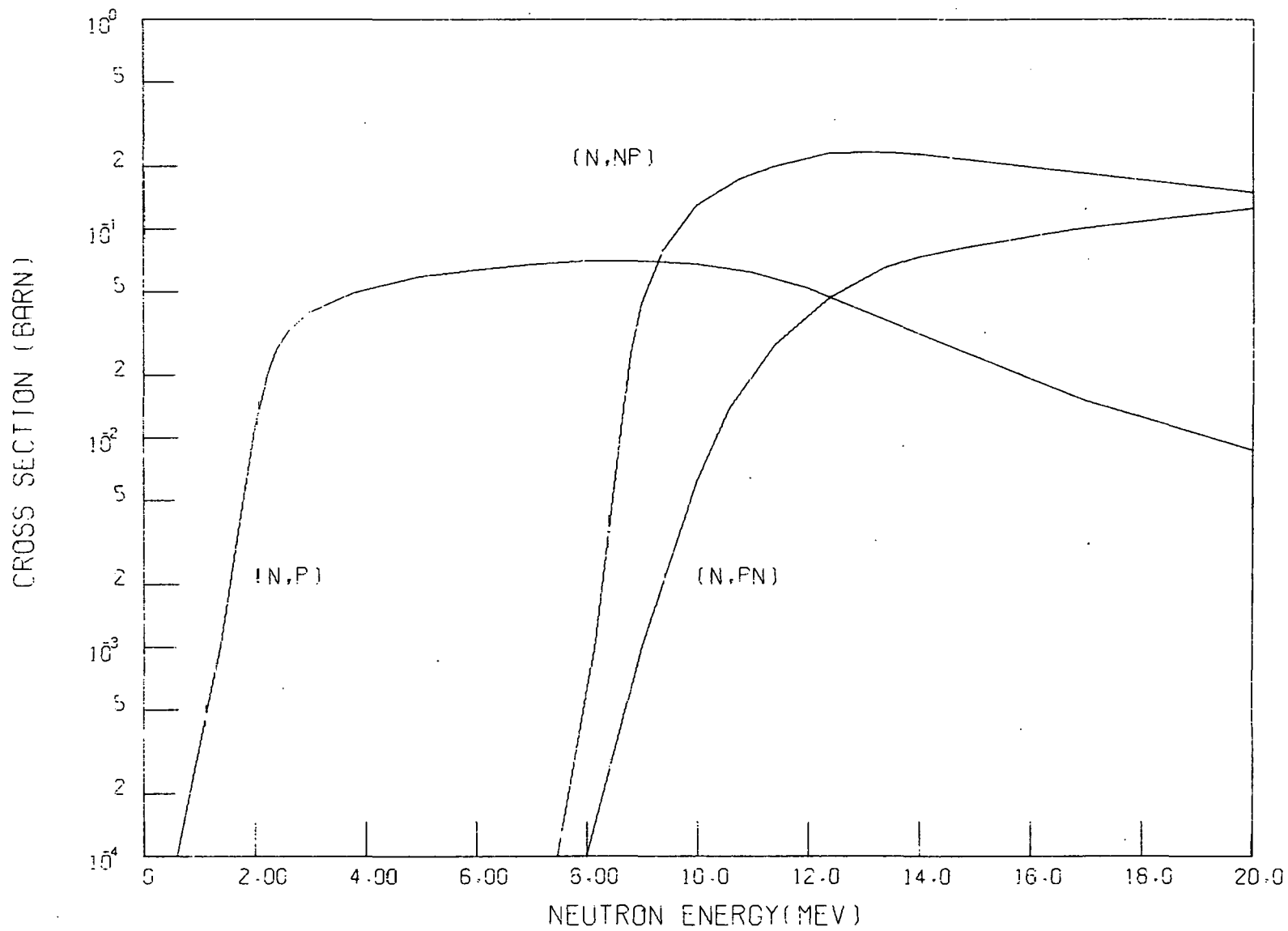
Fig. 6. Present evaluation of the (n,p), (n,np), and (n,pn) cross sections for [63]Cu.

23-FEB-79

For the ^{65}Cu(n,p) cross section, the previous evaluation was adopted.[31] The available data remained unchanged but appeared adequate to define the entire excitation function. For ^{65}Cu(n,np), the calculated results by Mann and Schenter[35] were adopted, but the cross sections above 12 MeV (20% at 20 MeV) were reduced to obtain agreement with the LLNL proton production cross section at 14.8 MeV. These results are shown in Fig. 7.

The cross-section values for the above reactions obtained for ^{63}Cu and ^{65}Cu, with abundances of 69.2% and 30.8% respectively, were combined for natural copper. The results are shown in Figs. 8 and 9 together with the ENDF/B-IV values.

5.2 (n,α) AND THE ALPHA-PARTICLE PRODUCTION CROSS SECTIONS

The alpha-particle production cross section below 20 MeV in copper is the sum of (n,α), (n,nα), and (n,αn) cross sections, or the sum of MT22 and MT107 in terms of the ENDF/B terminology. Here MT22 is the sum of (n,nα) and (n,αn) cross sections.

Two high-quality measurements for the alpha production cross section at 14.8 MeV have been made since the ENDF/B-IV evaluation. The LLNL measurements by Grimes et al.[34] were for ^{63}Cu and ^{65}Cu; the Rockwell measurement by Farrar and Kneff[35] was for natural copper. A weighted average of the LLNL data yielded 43 ± 7 mb for natural copper. The Rockwell value is 51 ± 3 mb. The average of the two values is 49 ± 2 mb. Weighing the original LLNL values for the isotopes by the last average, 64 mb for ^{63}Cu and 15 mb for ^{65}Cu were obtained. These values were used for normalization at 14.8 MeV in the following manner.

The ^{63}Cu(n,α) cross sections[37] evaluated for the ENDF/B-IV dosimetry file were adopted. The corresponding evaluation for the ENDF/B-V dosimetry file was not available at the time. The calculated excitation function for the sum of (n,nα) and (n,αn) cross sections[9] was normalized to yield the required alpha production cross section of 64 mb at 14.8 MeV. These cross sections are shown in Fig. 10.

For ^{65}Cu, the sum of (n,nα) and (n,αn) cross sections was unchanged from the earlier evaluation[31] which had adequate data. For ^{65}Cu(n,α), the calculation by Mann and Schenter[35] was used up to 12 MeV, and their calculated curve above 12 MeV (40% reduction near 15 MeV) was reduced to obtain
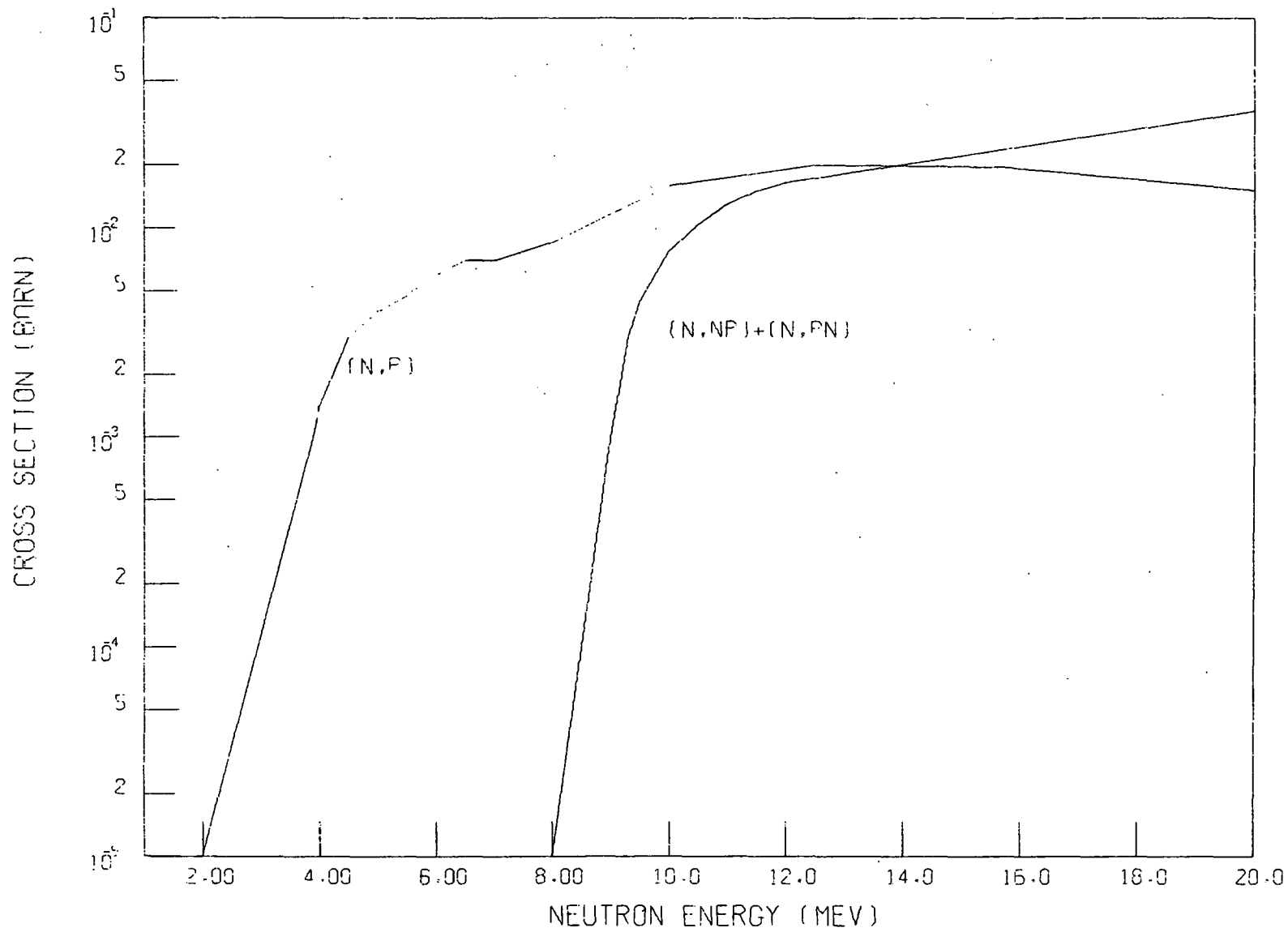
Fig. 7. Present evaluation of (n,p), (n,pn) + (n,np) cross sections for ^{65}Cu. ^{65}Cu(n,p) cross sections were taken from the previous evaluation[31] where adequate data existed.
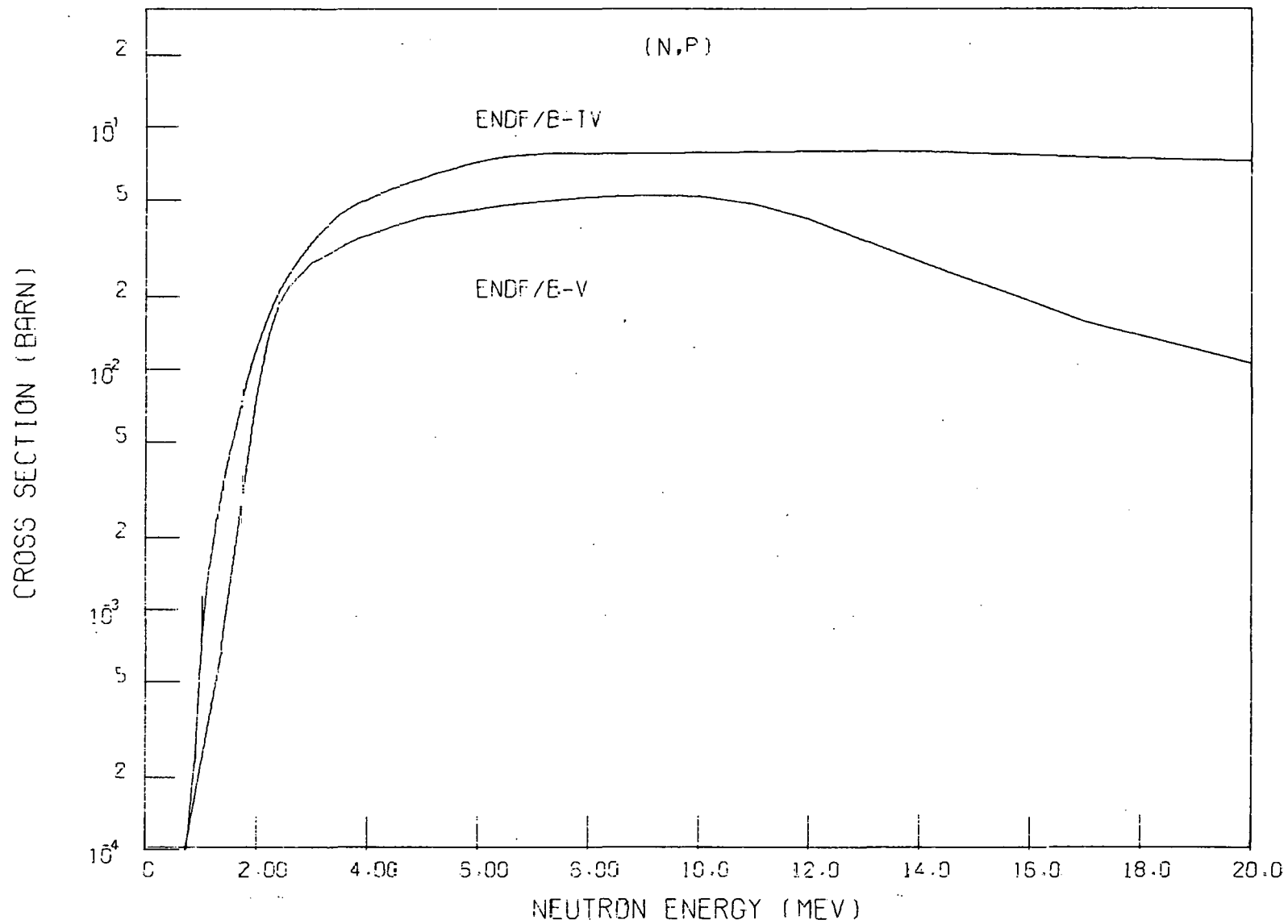
Fig. 8. Comparison of ENDF/B-V (n,p) cross sections with ENDF/B-IV for natural copper.
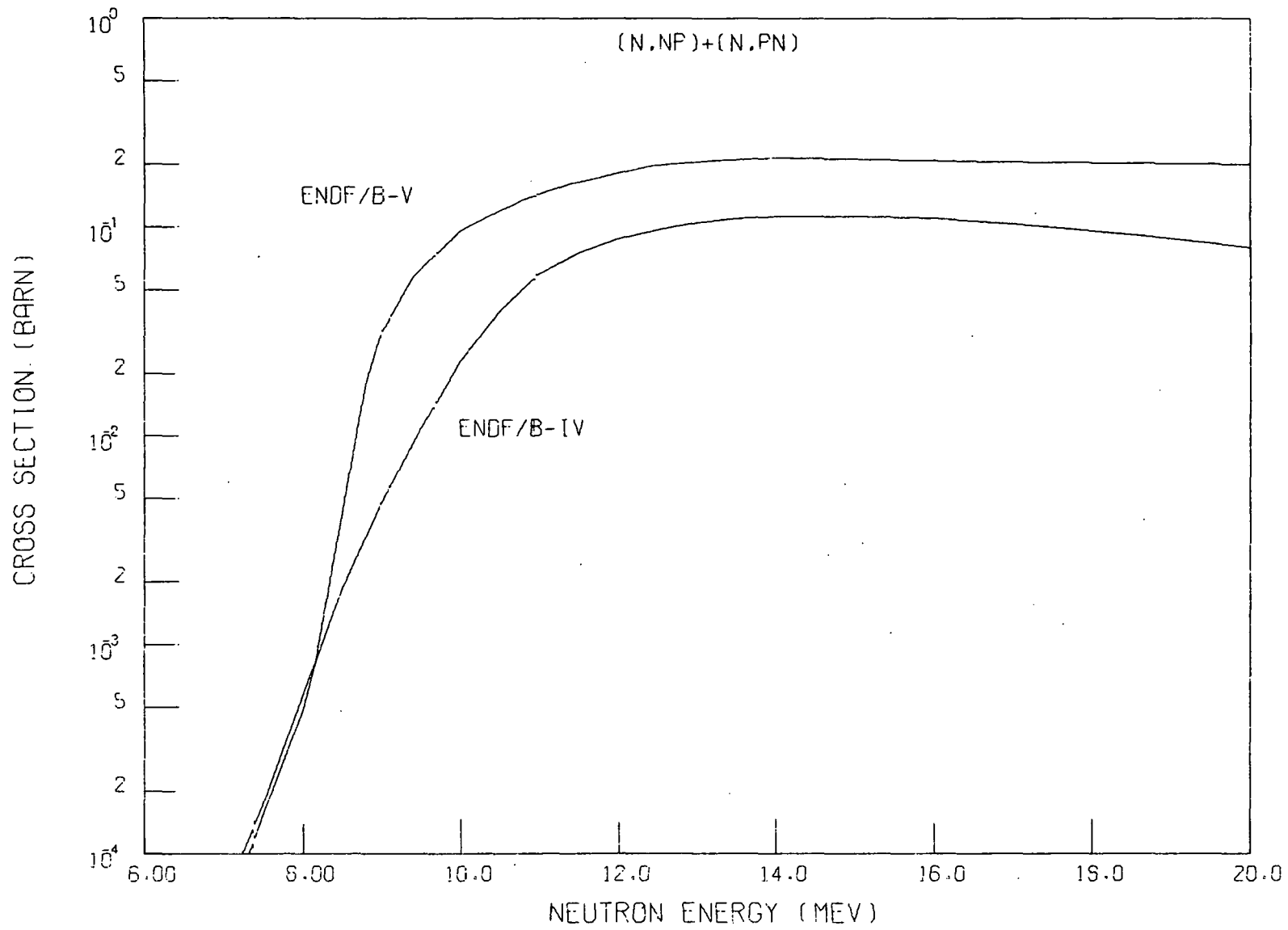
Fig. 9. Comparison of ENDF/B-V (n,pn) + (n,np) cross sections with ENDF/B-IV for natural copper.

CROSS SECTION (BARN)

10^0

5

2

10^{-1}

5

2

10^{-2}

5

2

10^{-3}

5

2

10^{-4}

(N,NA)+(N,AN)

(N,A)

0   2·00   4·00   6·00   8·00   10·0   12·0   14·0   16·0   18·0   20·0

NEUTRON ENERGY (MEV)
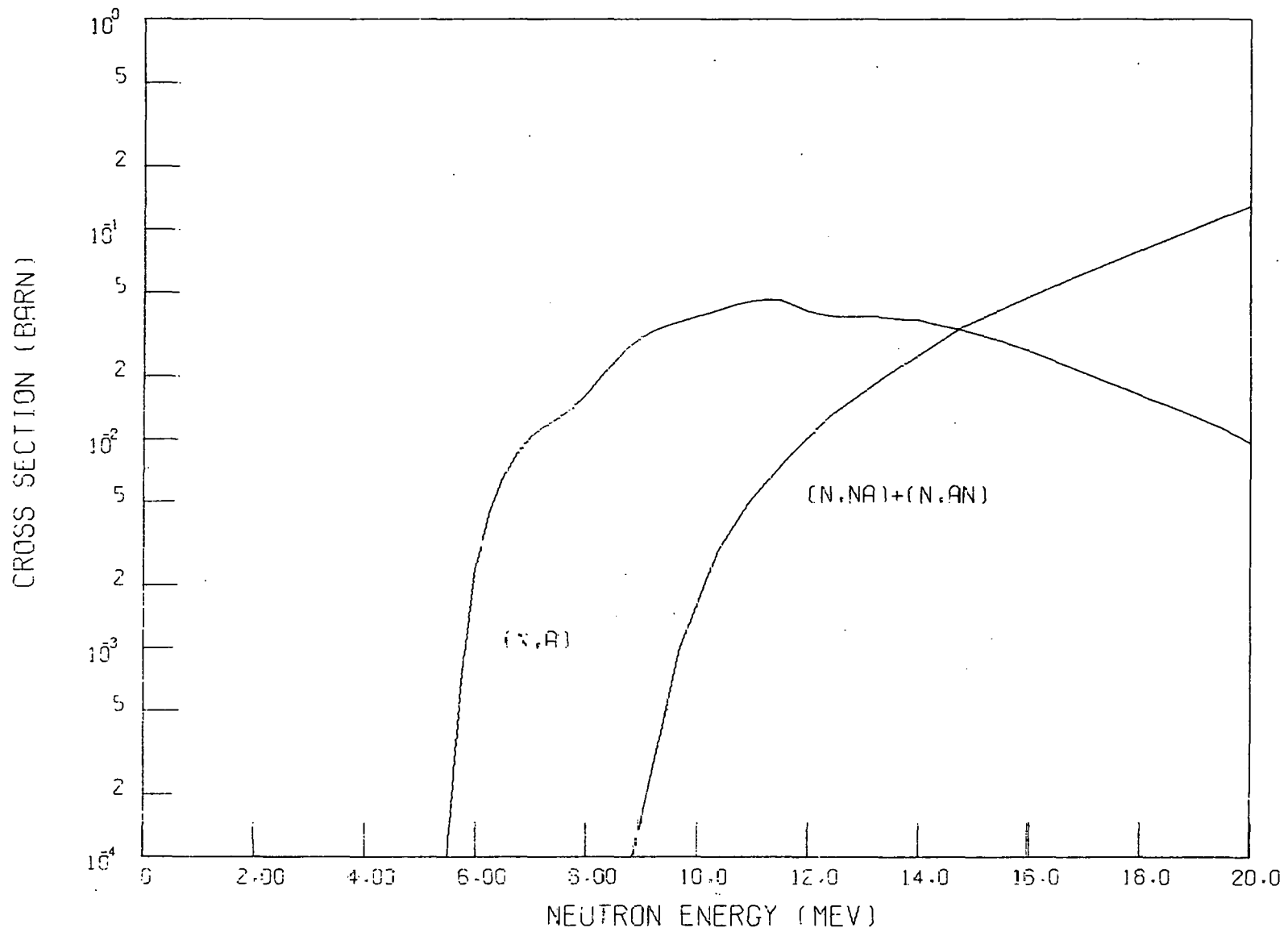
Fig. 10. Present evaluation of (n,α) and (n,αn) + (n,nα) cross sections for [63]Cu. [63]Cu(n,α) cross sections were taken from the ENDF/B-IV dosimetry file.[37]

the required 14.8-MeV value for the alpha production cross section. The results are shown in Fig. 11.

The results recommended for natural copper are shown in Figs. 12 and 13 together with those for ENDF/B-IV.

5.3 TOTAL CROSS SECTIONS

The high-resolution total cross sections from 80 keV to 20 MeV measured by Perey[38] using the Oak Ridge Electron Linear Accelerator (ORELA) were compared with the ENDF/B-IV values and some older data.[39-41] The ORELA data shown in Figs. 14 to 25 were fitted by line segments and were adopted for Version V because high-resolution total cross sections were needed for shielding applications. However, the agreement of the data as shown in Figs. 14 to 25 is generally poor. The ORELA data were adopted after it was observed that ORELA total cross sections for other materials which were measured similarly in the same energy range have been found to agree with high-resolution data taken elsewhere.[1,3,10] From 2 to 20 MeV, there was good agreement between the ORELA data and the ENDF/B-IV values as shown in Fig. 26. In Fig. 27 the available total cross sections from 80 keV to 200 keV are shown. It appears there is a gap between 100 keV and 200 keV where high-resolution total cross sections are needed.

5.4 CAPTURE GAMMA-RAY SPECTRA

The gamma-ray production cross sections and spectra measured by Chapman et al.[42] using ORELA for two incident neutron bins from 0.2 to 0.6 MeV and from 0.6 to 1.25 MeV were adopted. These were given in the evaluated file as capture gamma rays after removing the contributions from inelastic scattering as shown in Figs. 28 and 29. There were no other data available in this energy range. For higher incident neutron energies, the ORELA data and the ENDF/B-IV values appeared[42] in good agreement.

5.5 THINNING OF CAPTURE CROSS SECTIONS

The capture cross sections in the ENDF/B-IV evaluation were thinned to 1% linearly, reducing the energy entries from 408 to 48. This automatically shortened the files for total, elastic, and nonelastic cross sections.
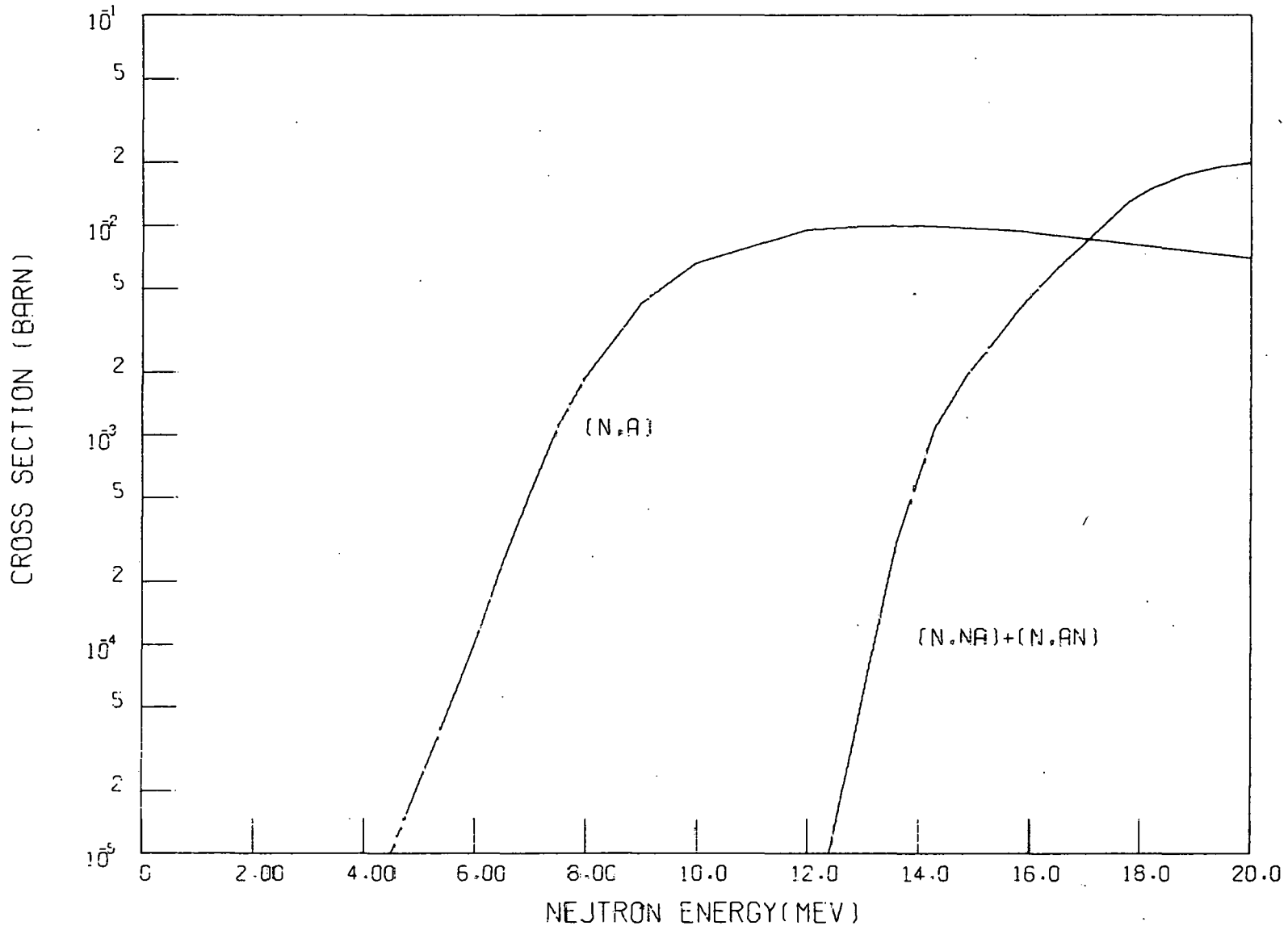
Fig. 11. Present evaluation of (n,α) and (n,nα) + (n,αn) cross sections for ^{65}Cu.
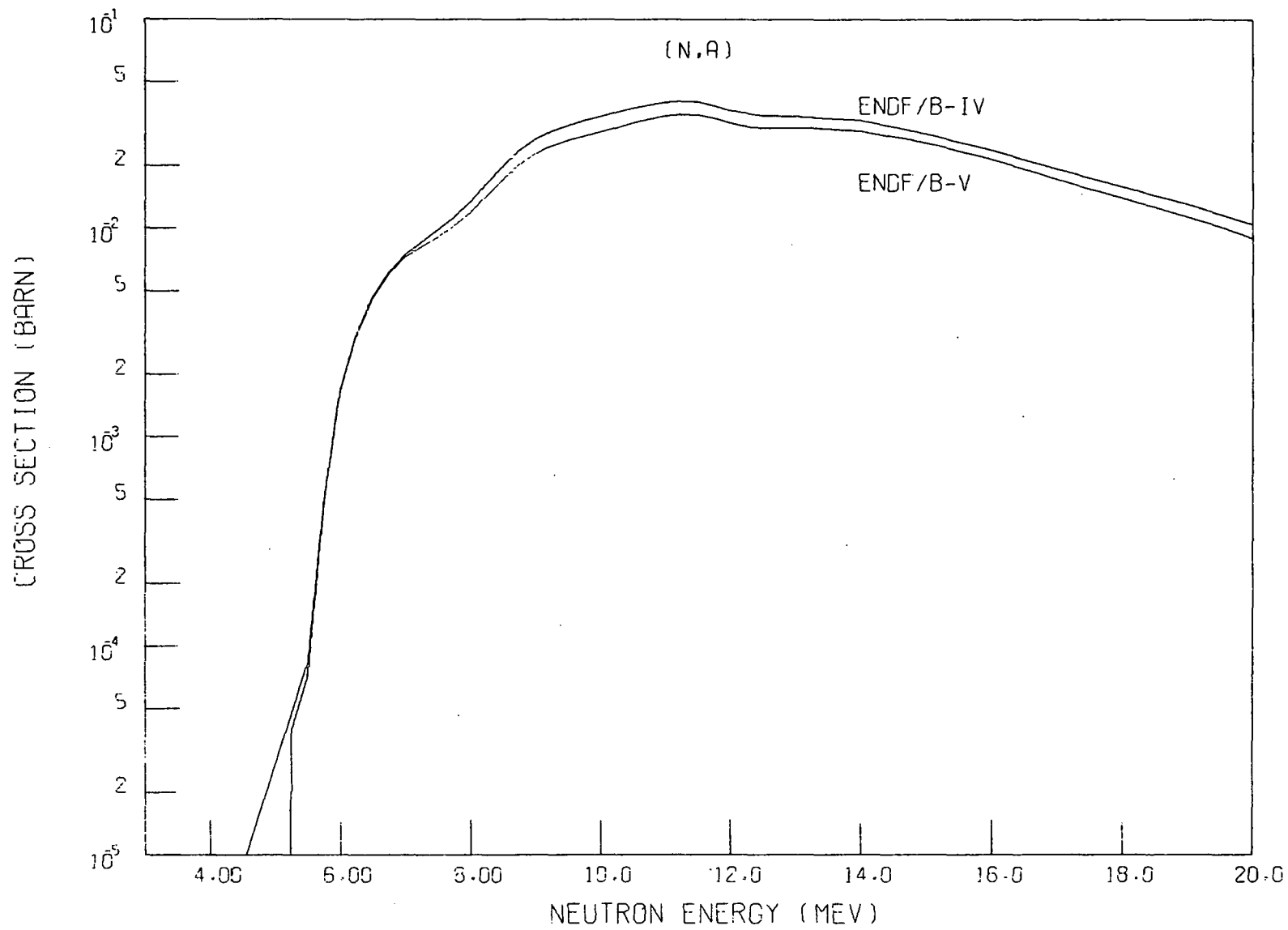
Fig. 12. Comparison of ENDF/B-V (n,α) cross sections with ENDF/B-IV for natural copper.
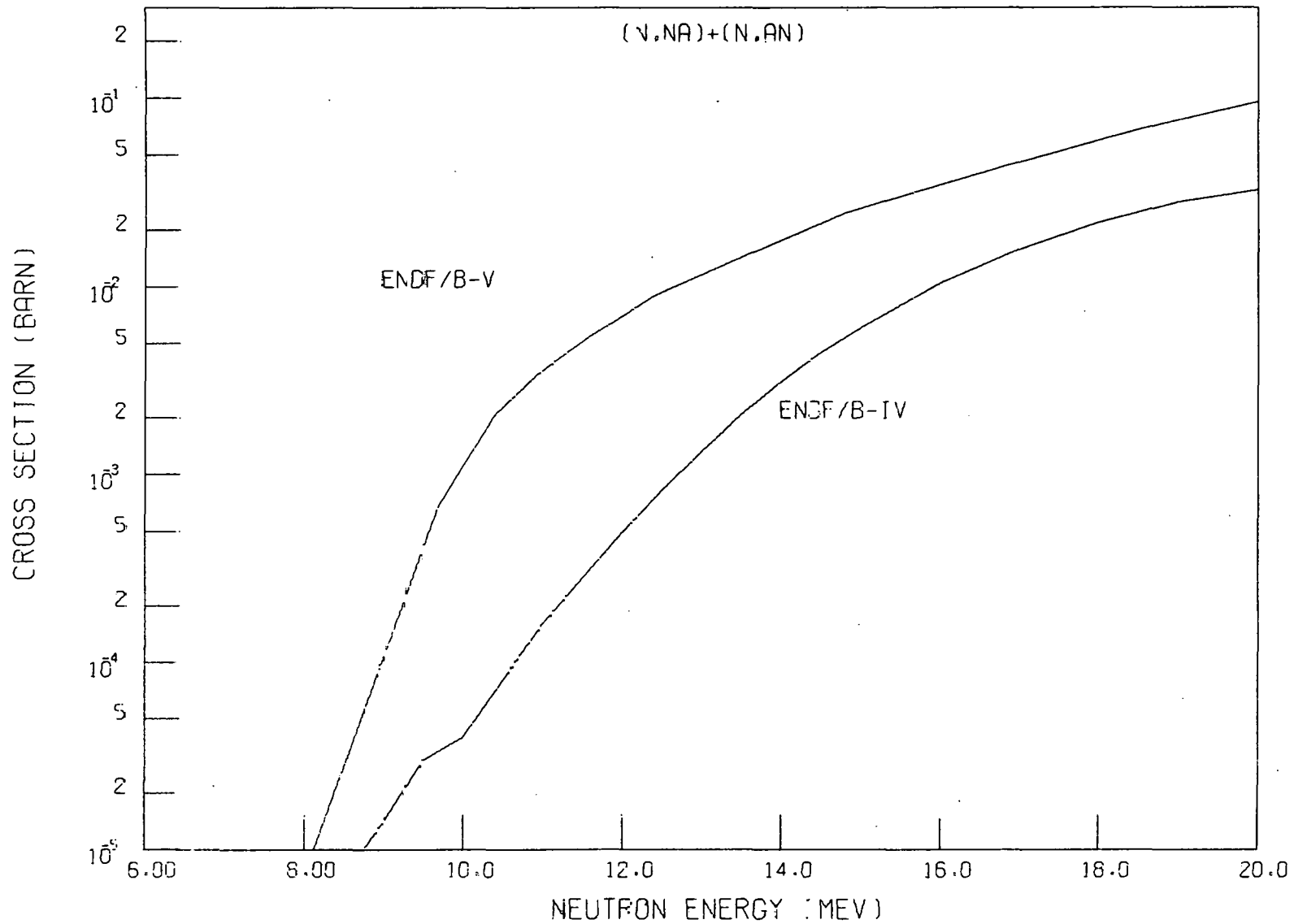
Fig. 13. Comparison of ENDF/B-V (n,αn) + (n,nα) cross sections with ENDF/B-IV for natural copper.
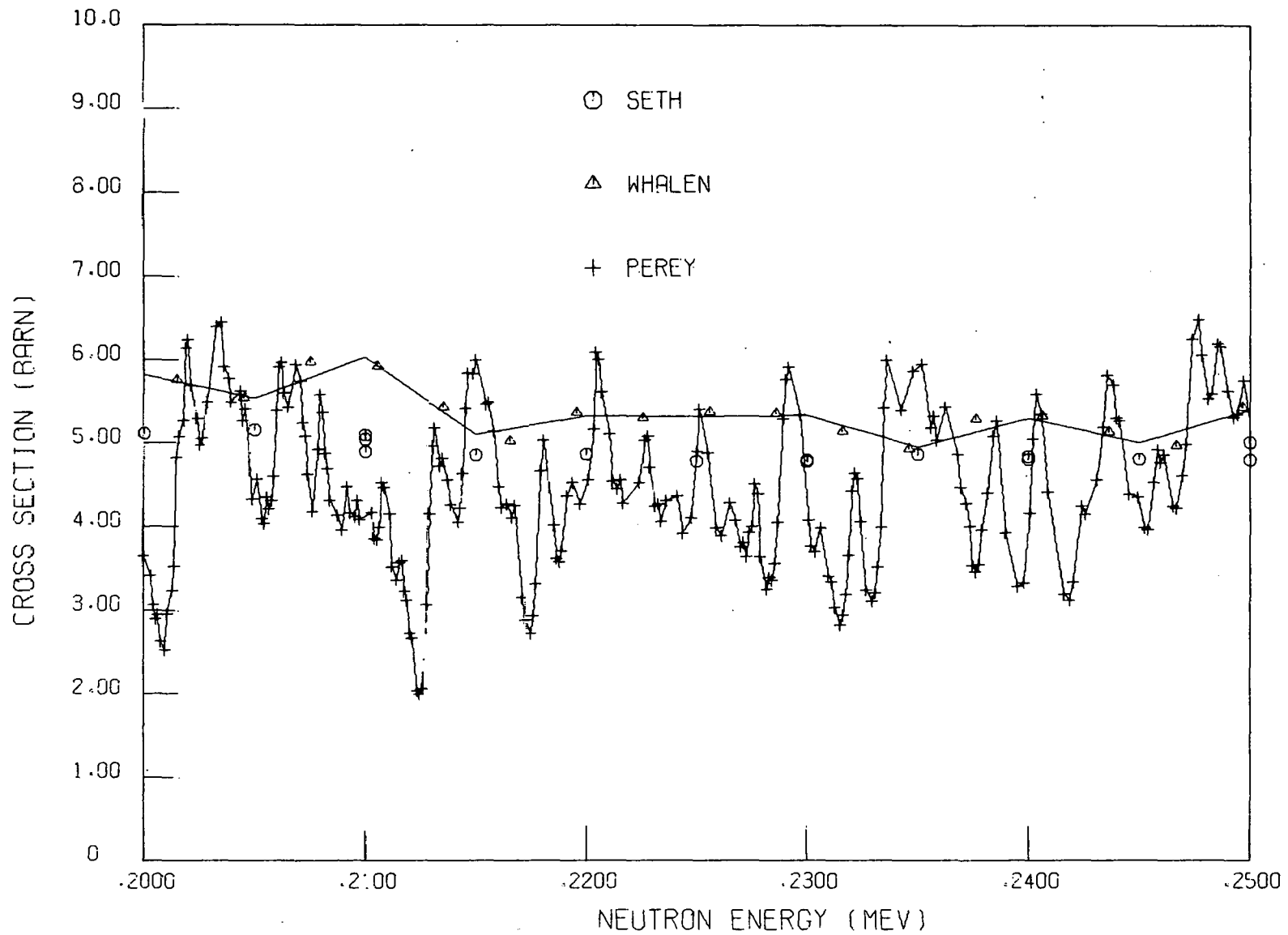
Fig. 14. Cu total cross sections in ENDF/B-IV and -V (Perey's data).

15-FEB-79
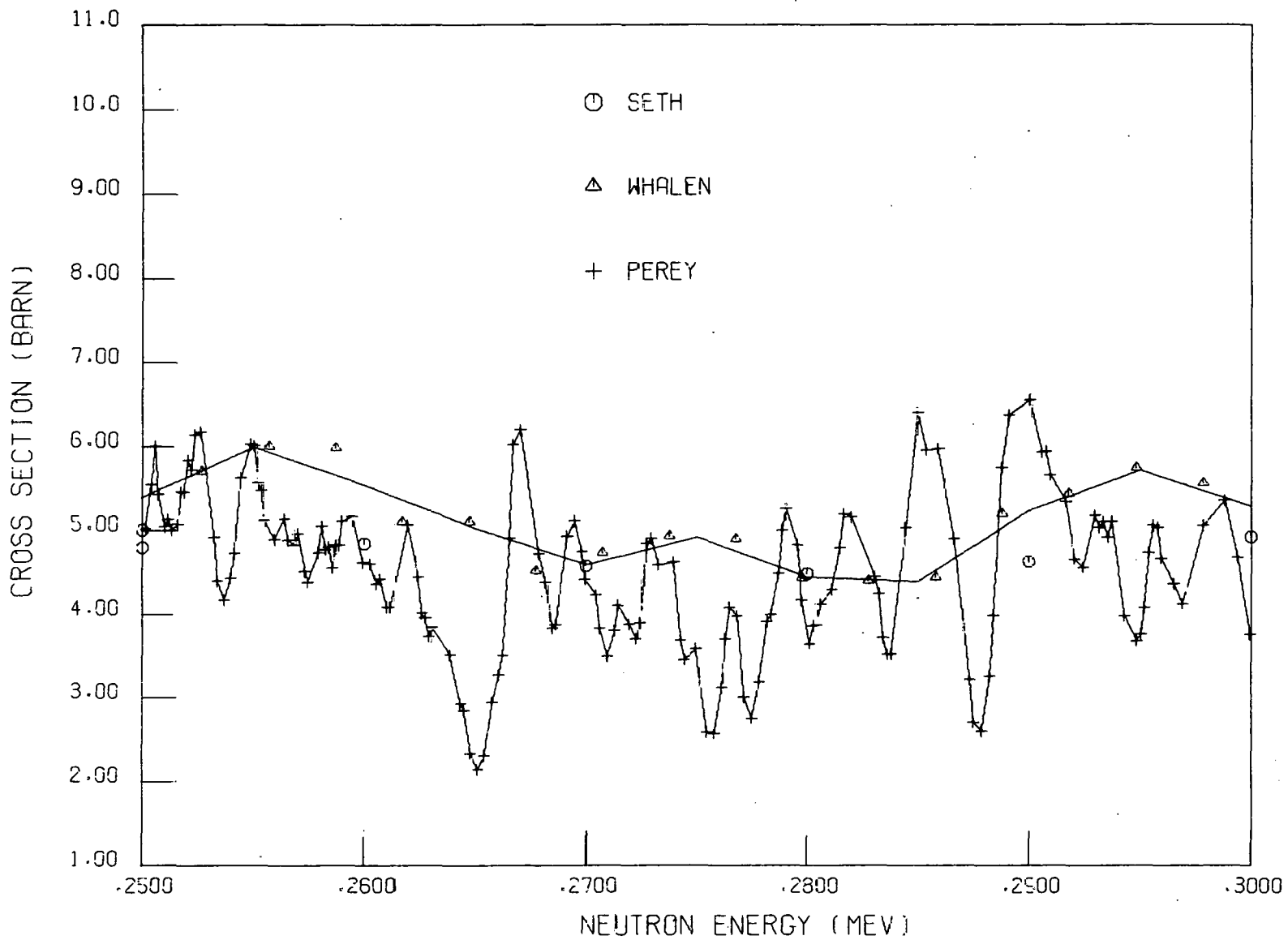
Fig. 15. Cu total cross sections in ENDF/E-IV and -V (Perey's data).

17-FEB-79
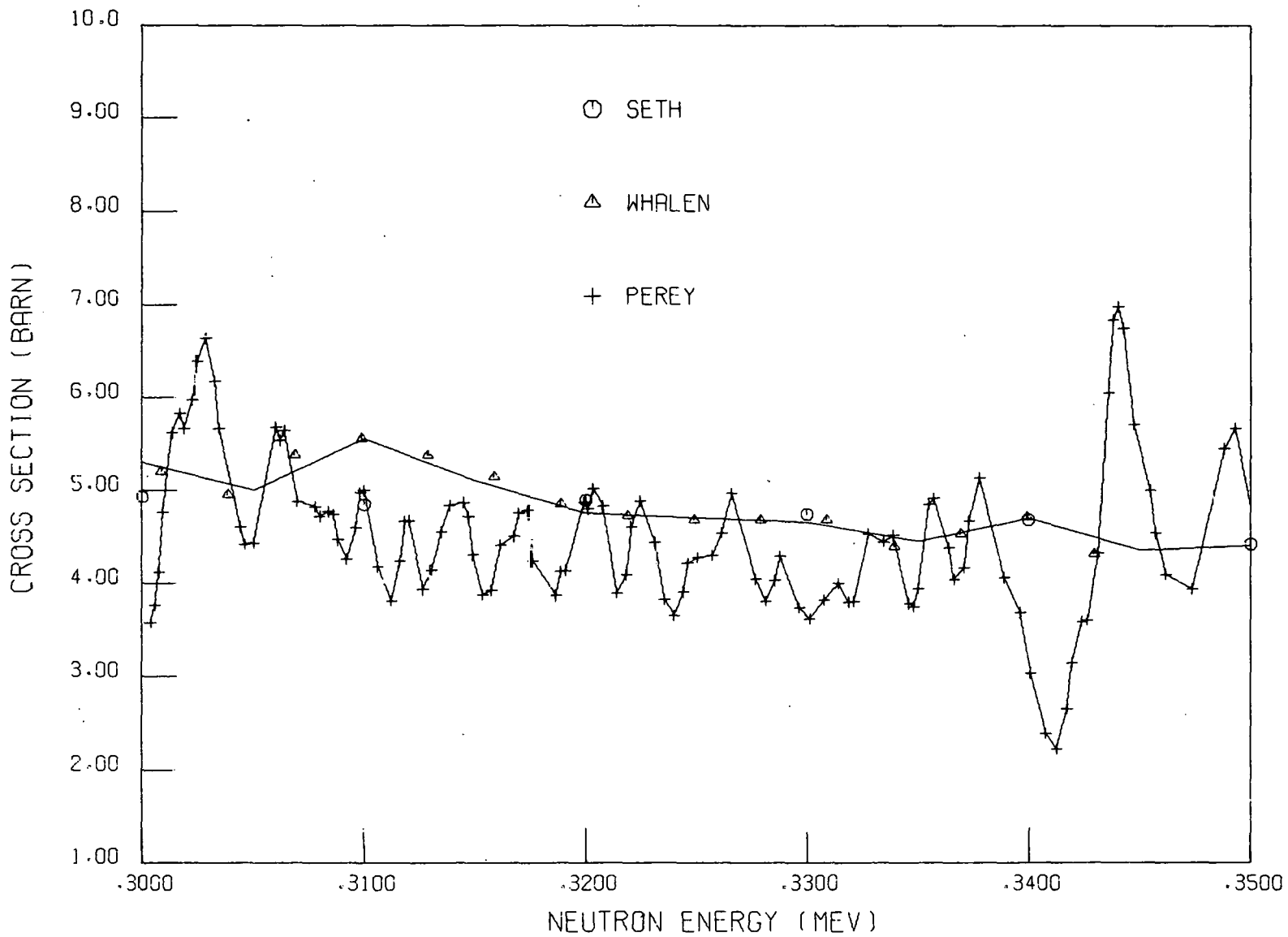
Fig. 16. Cu total cross sections in ENDF/B-IV and -V (Perey's data).
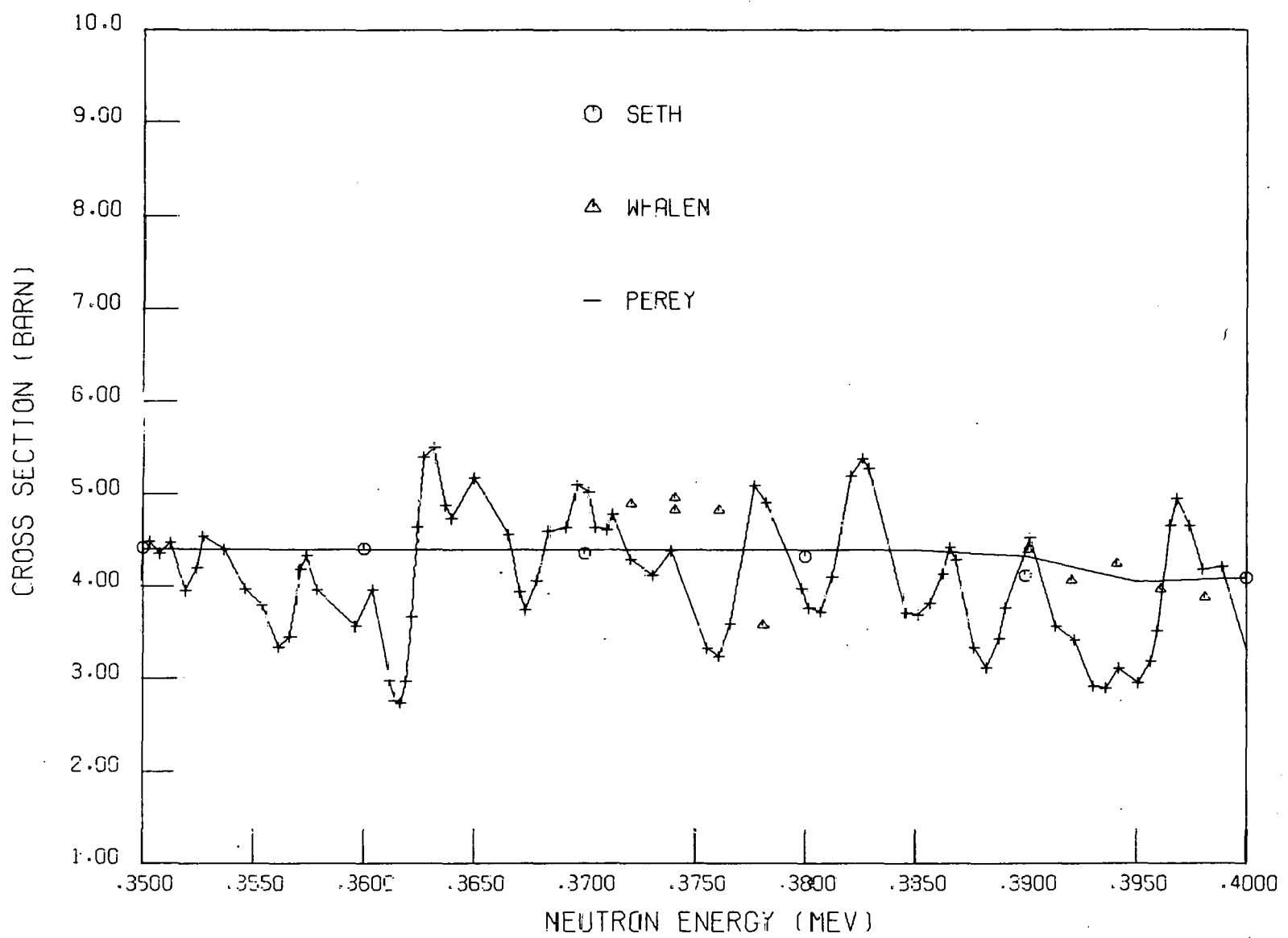
Fig. 17. Cu total cross sections in ENDF/B-IV and -V (Perey's data).
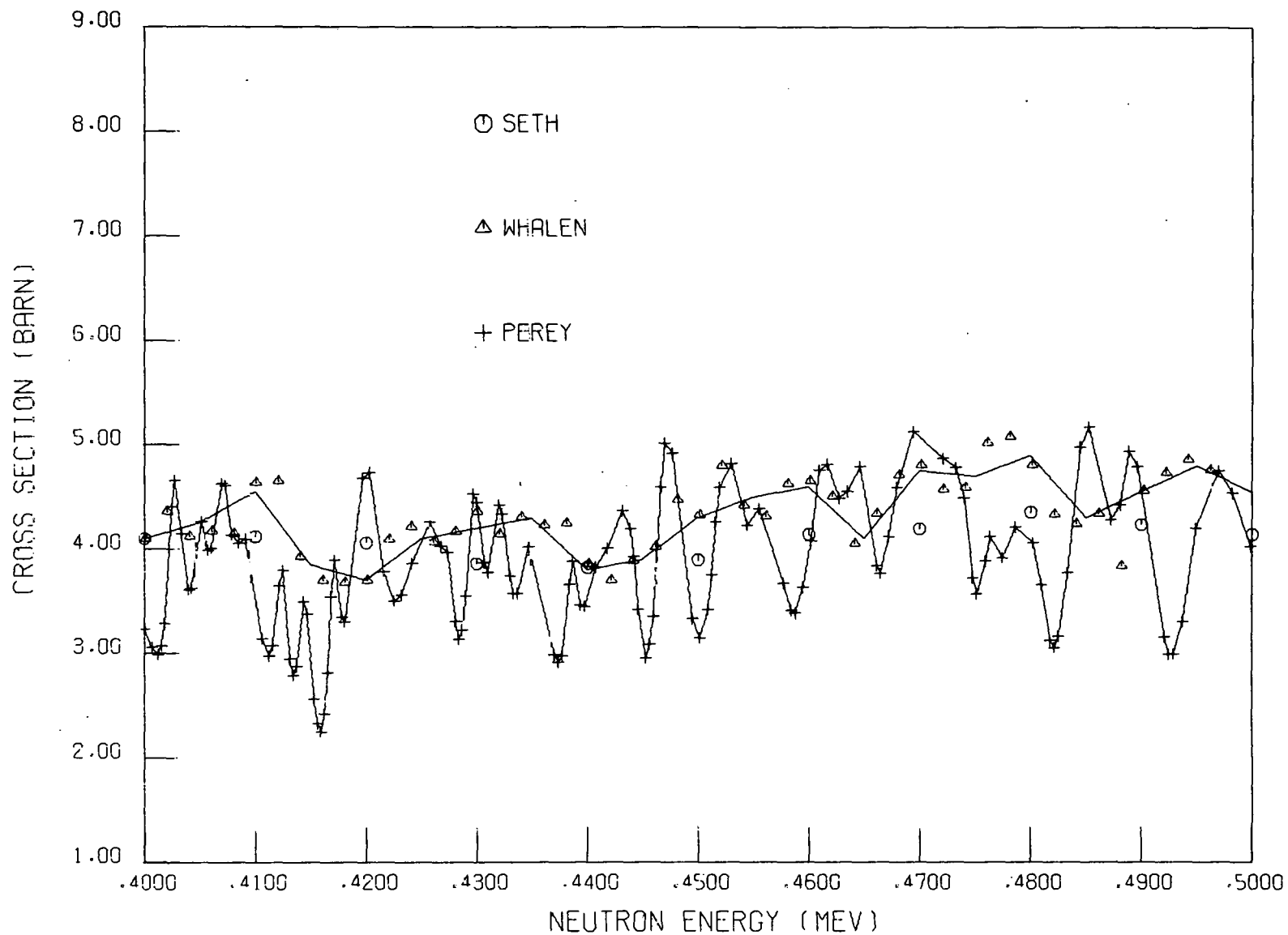
Fig. 18. Cu total cross sections in ENDF/B-IV and -V (Perey's data).

17-FEB-79
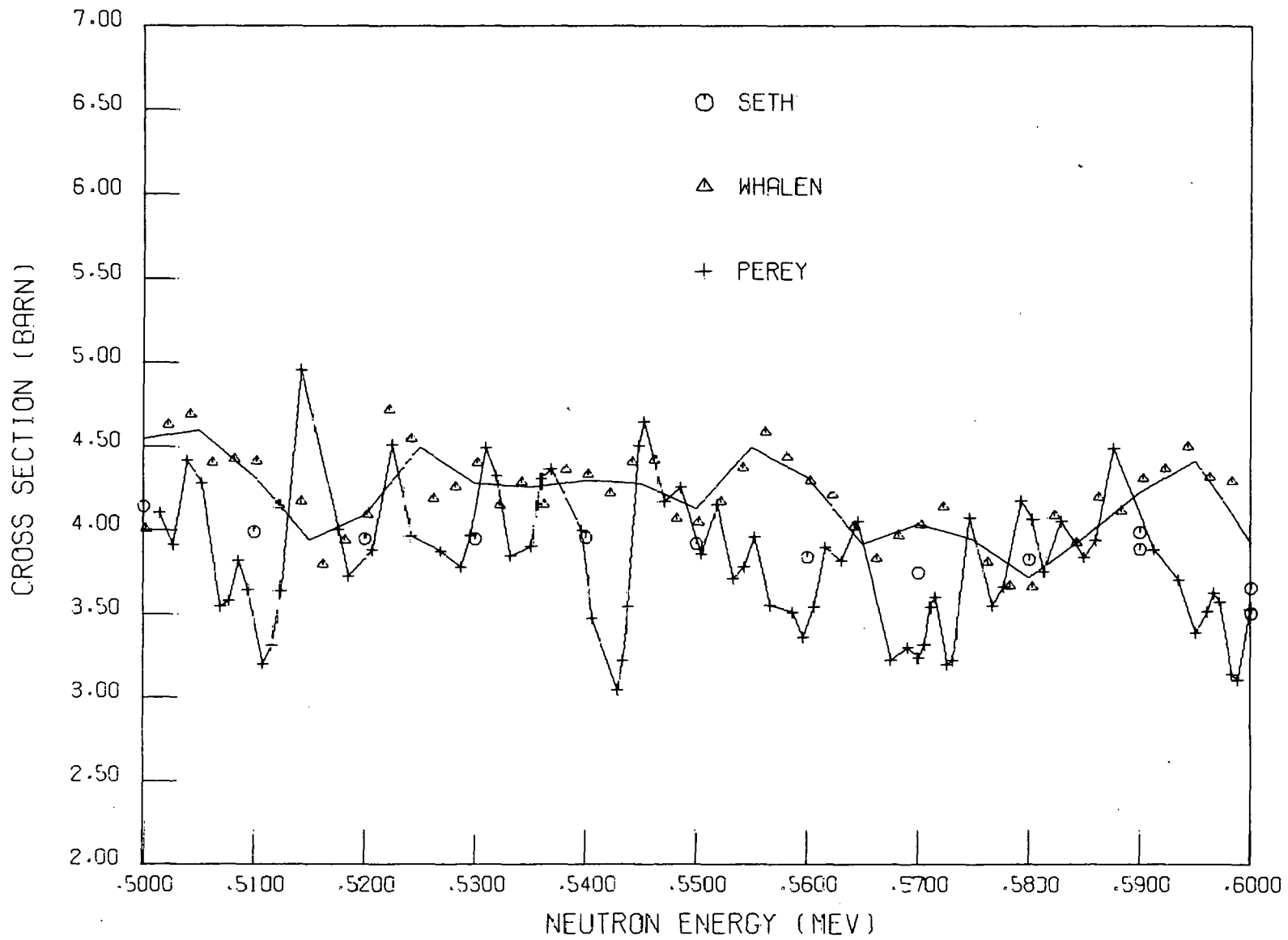
Fig. 19. Cu total cross sections in ENDF/B-IV and -V (Perey's data).

34
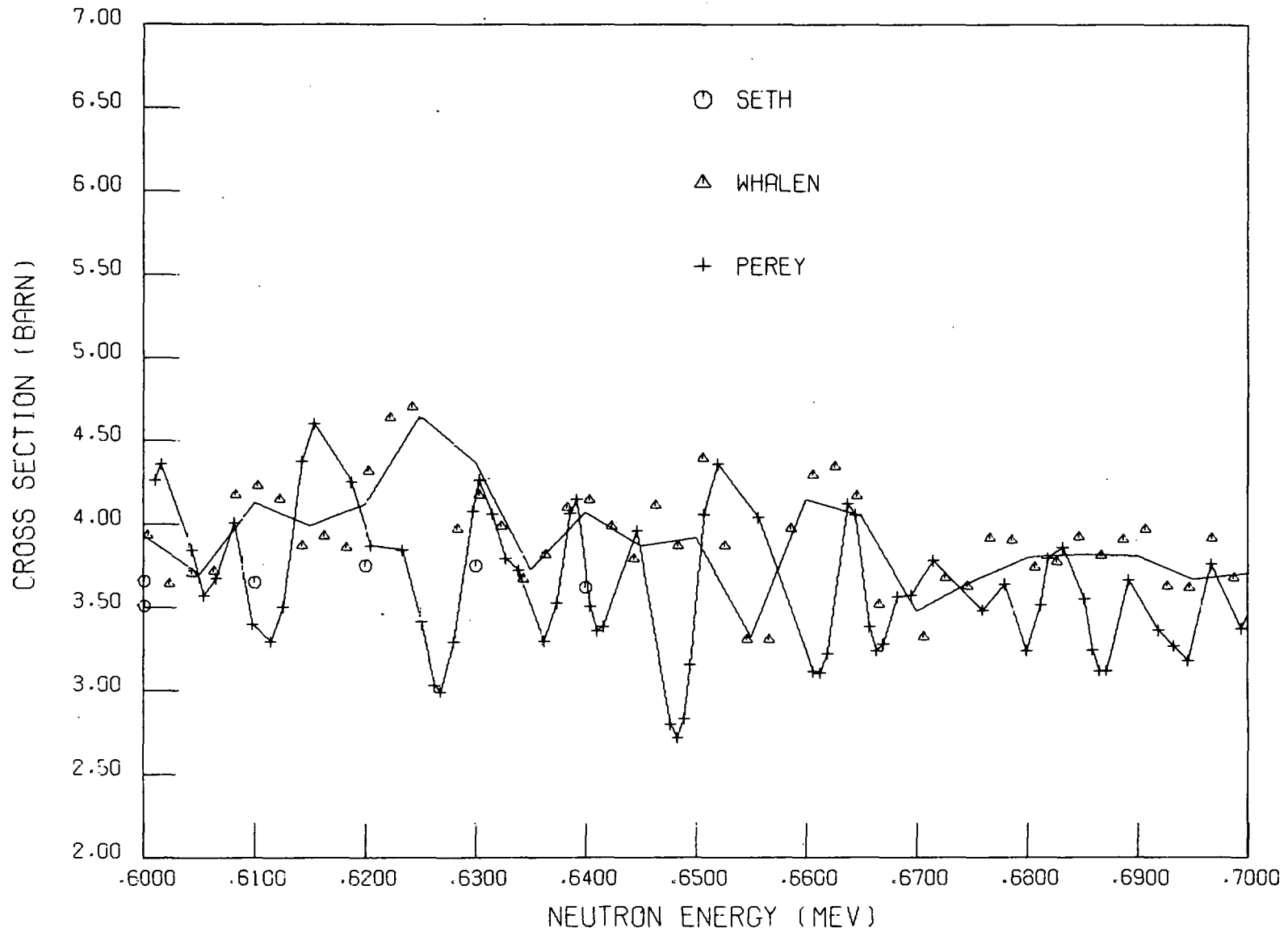
Fig. 20. Cu total cross sections in ENDF/B-IV and -V (Perey's data).

17-FER-73
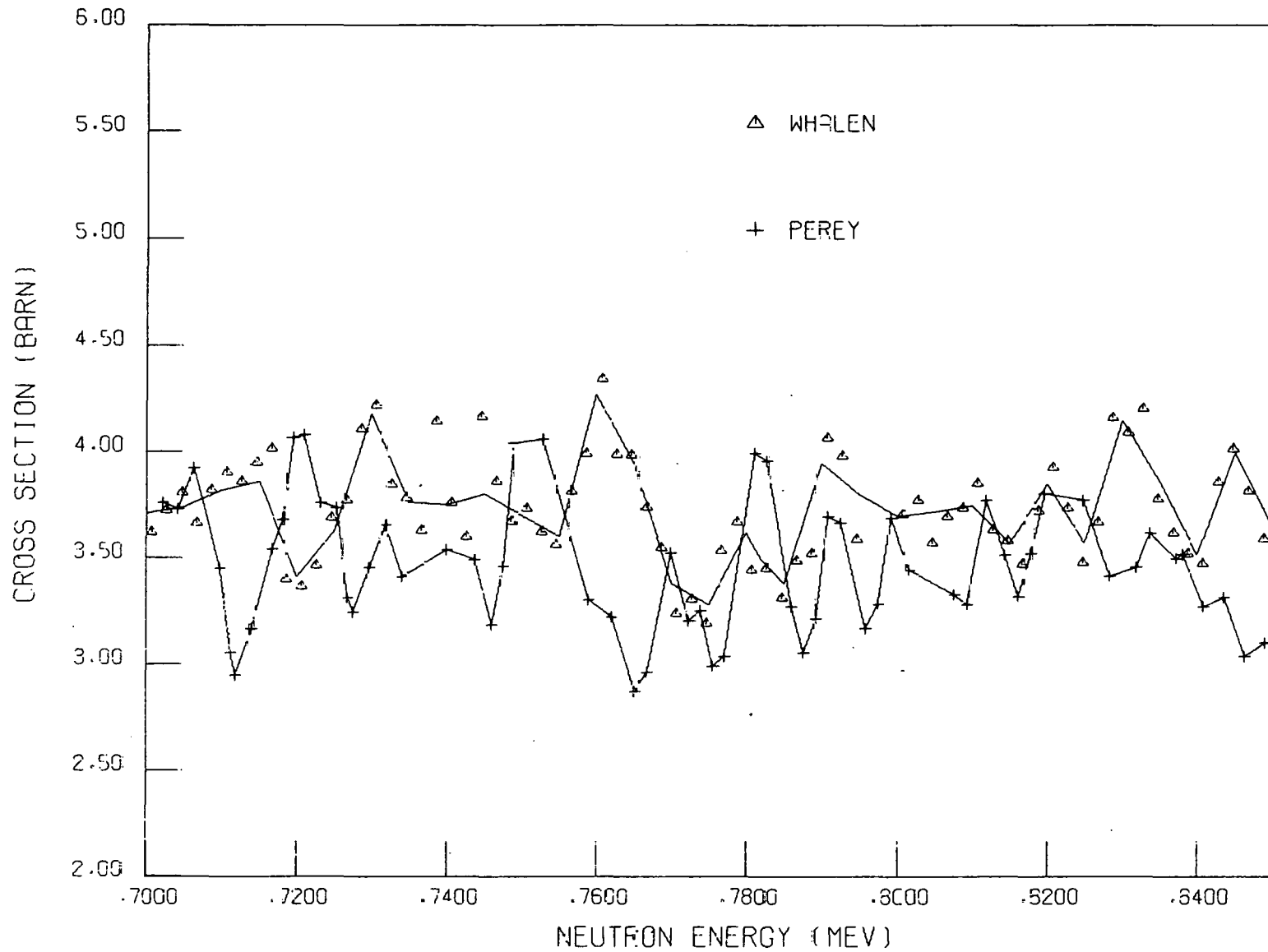
Fig. 21. Cu total cross sections in ENDF/B-IV and -V (Perey's data).

17-FEB-79

Fig. 22. Cu total cross sections in ENDF/B-IV and -V (Perey's data).

CROSS SECTION (BARN)

5.00

4.50

4.00

3.50

3.00

2.50

2.00

.6600   .6800   .9000   .9200   .9400   .9600   .9800   1.00

NEUTRON ENERGY (MEV)

△ WHALEN
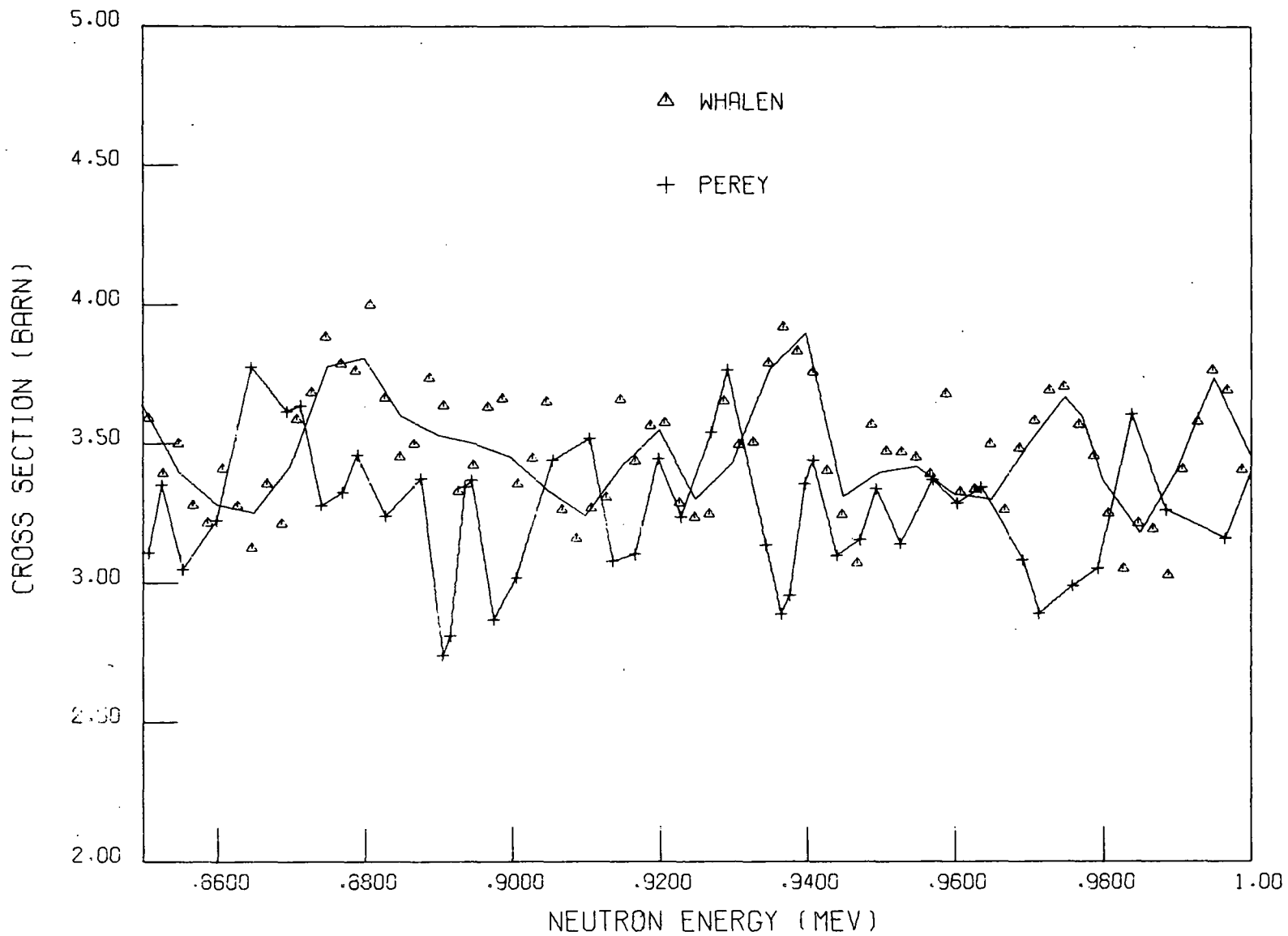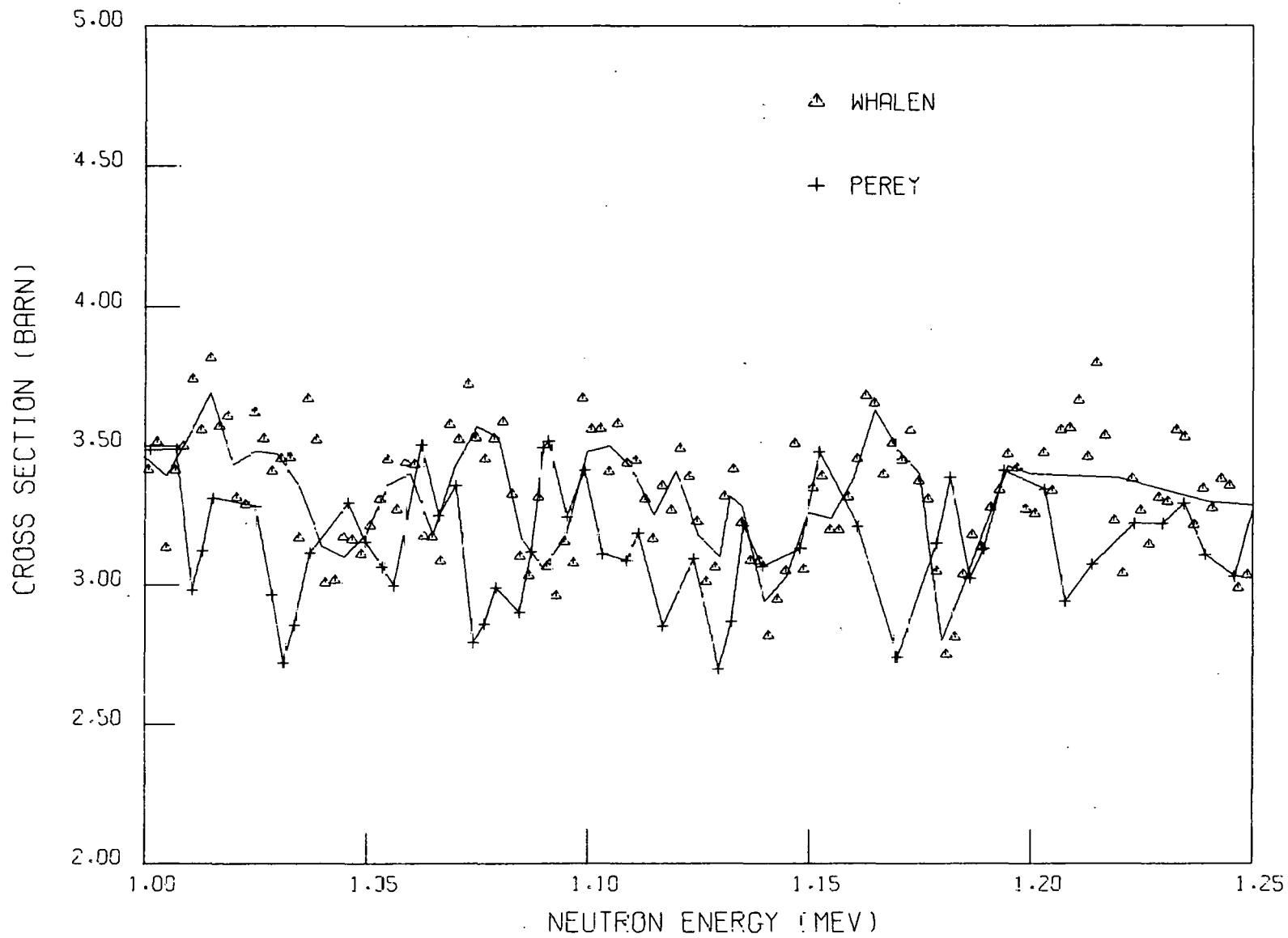
+ PEREY

Fig. 23. Cu total cross sections in ENDF/B-IV and -V (Perey's data).
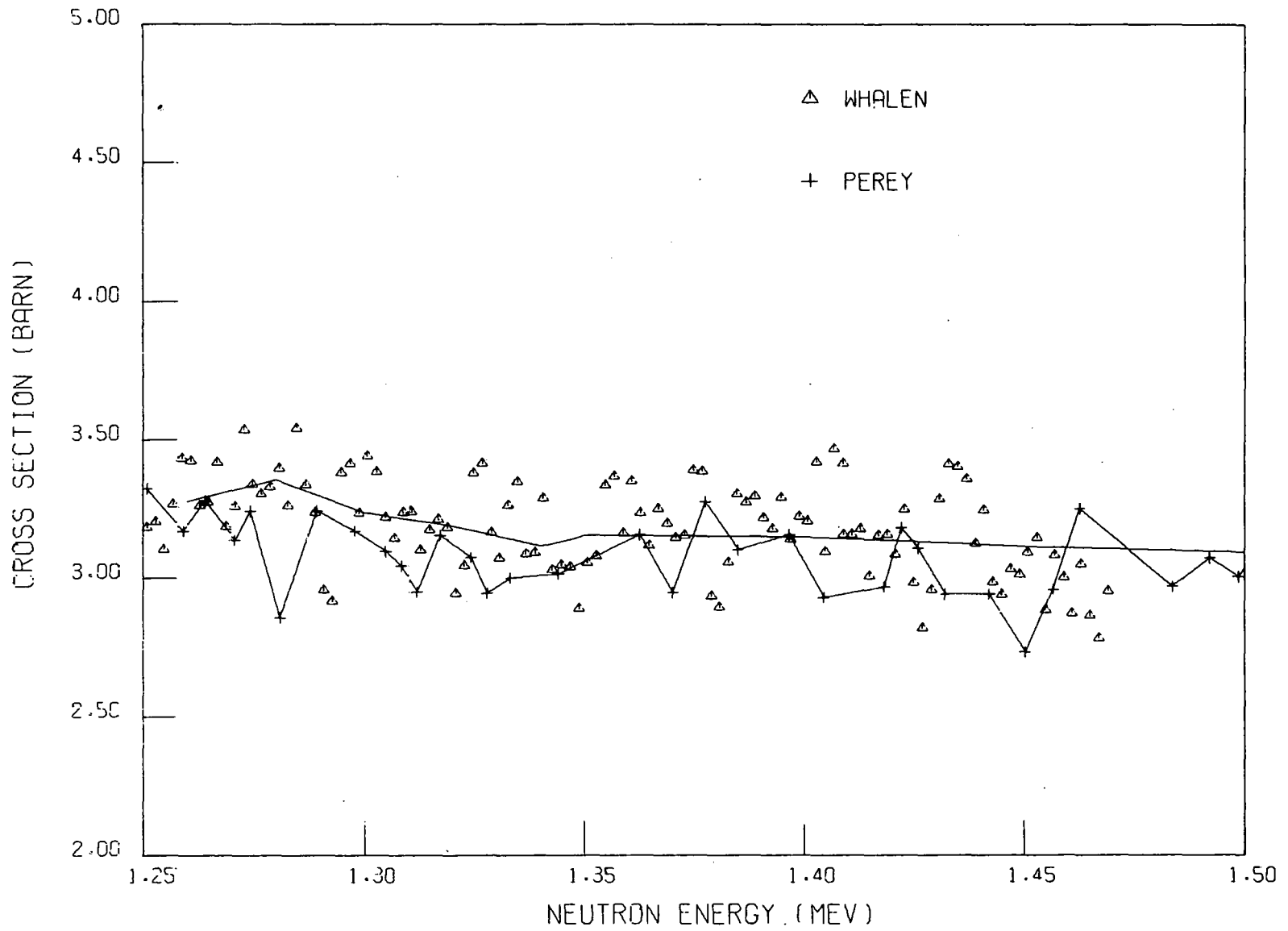
17-FEB-79

Fig. 24. Cu total cross sections in ENDF/B-IV and -V (Perey's data).

17-FEB-79
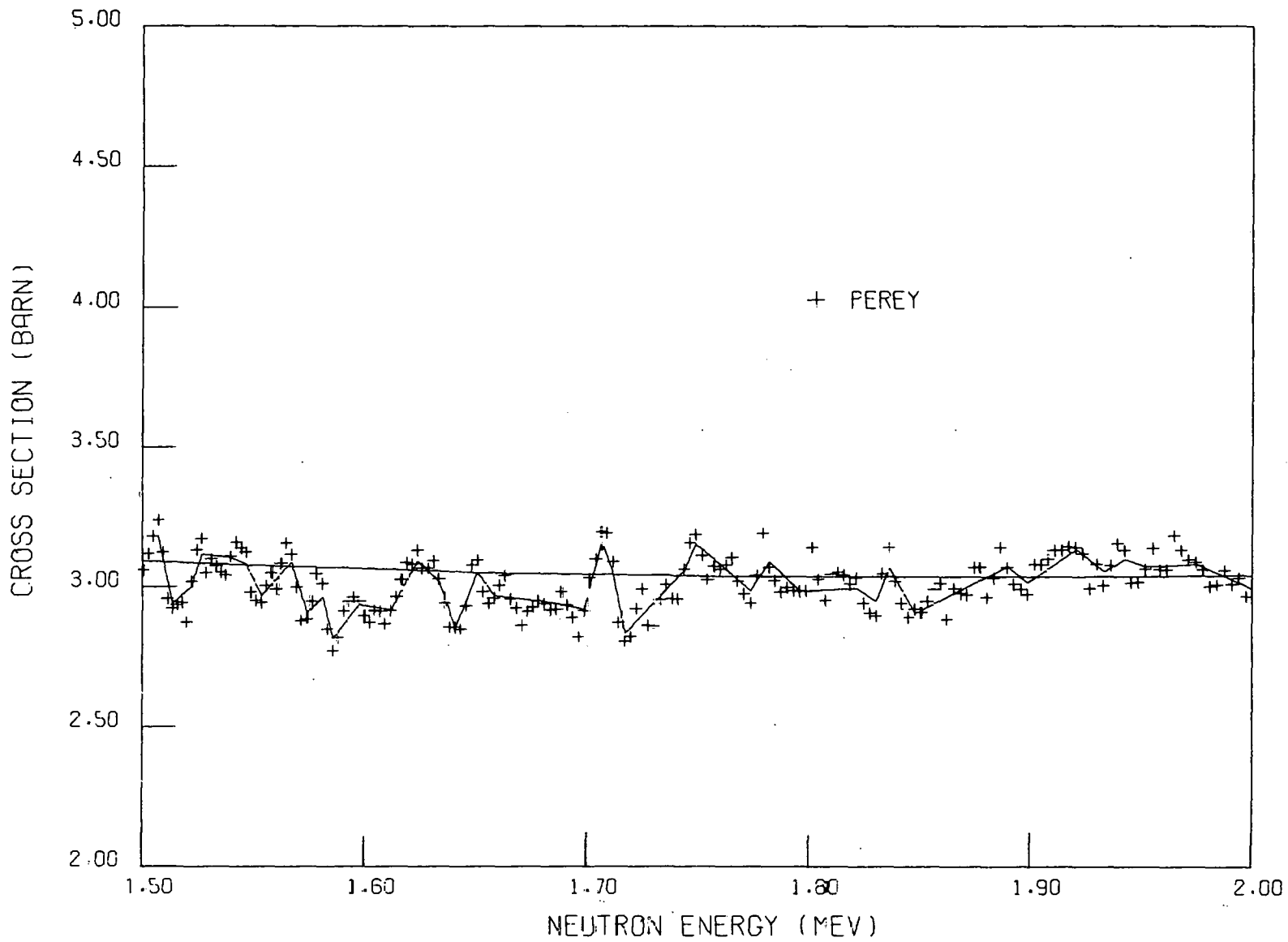
Fig. 25. Cu total cross sections in ENDF/B-IV and -V (Perey's data).
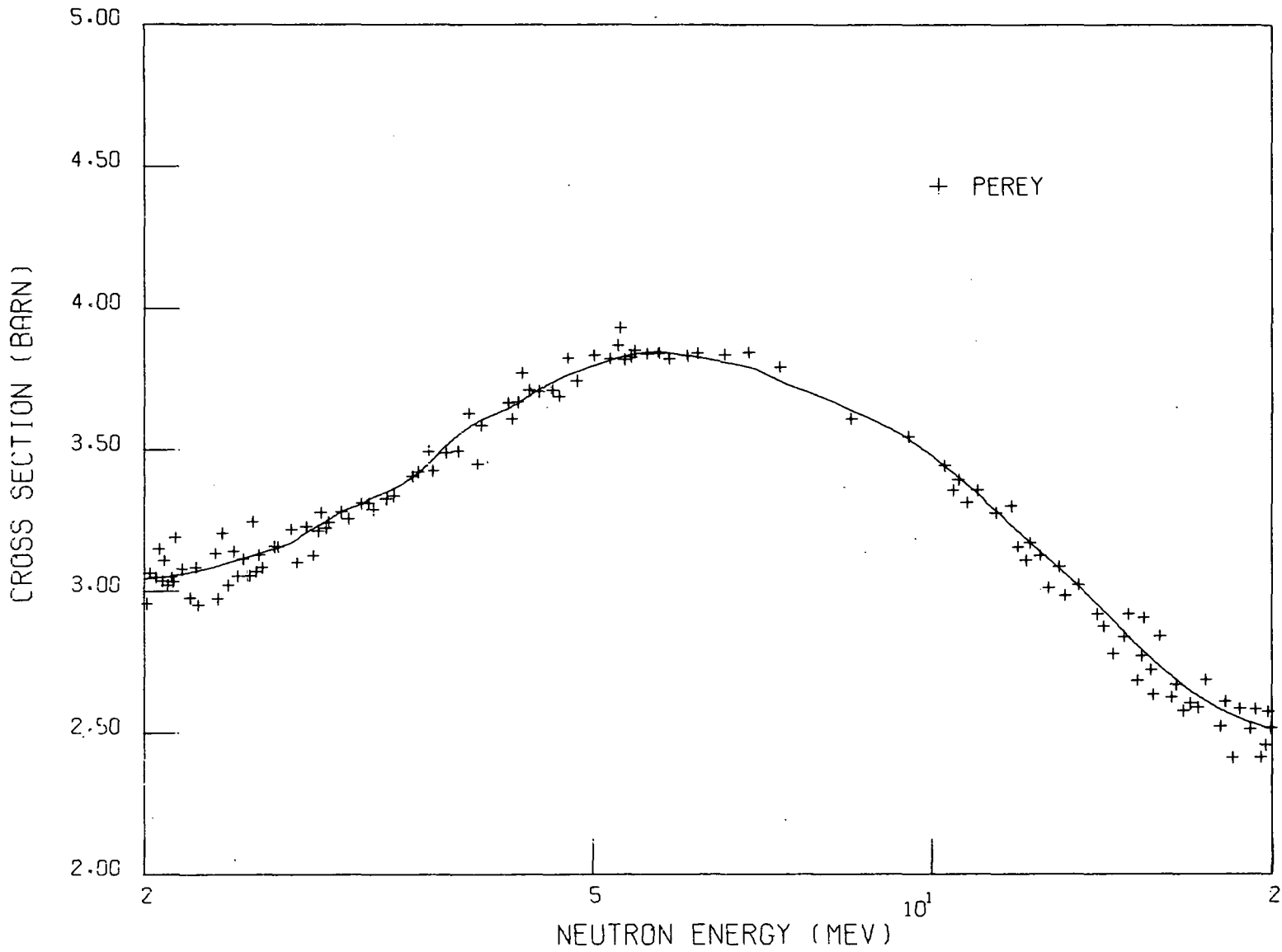
Fig. 26. Perey's measurement of total cross sections for Cu from 2.0 MeV to 20.0 MeV confirms the ENDF/B-IV evaluation.
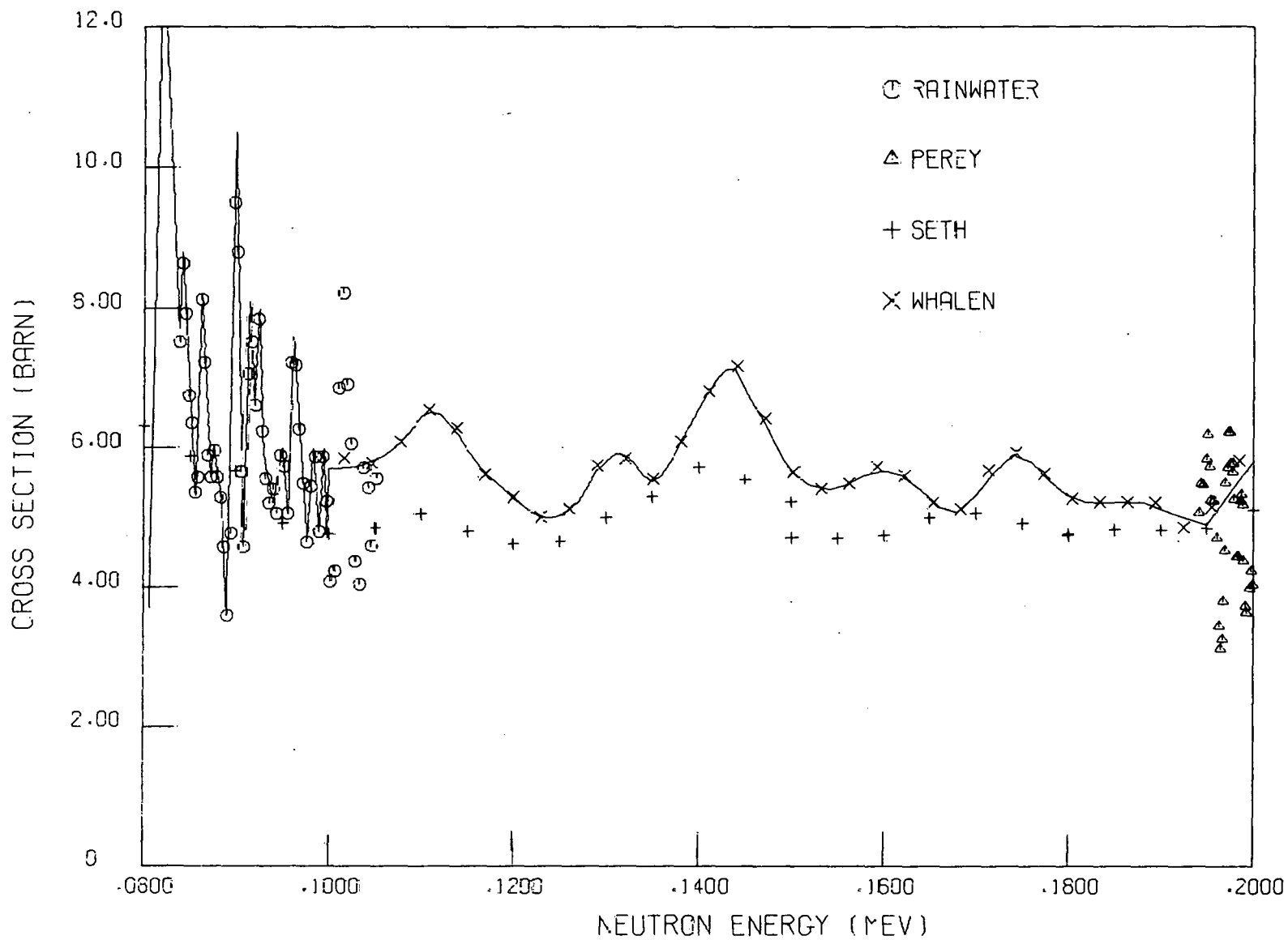
Fig. 27. A comparison of ENDF/B-IV evaluation of the total cross sections for Cu from 80 keV to 200 keV with the available data. A lack of adequate data between 100 keV and 200 keV seems to be indicated.
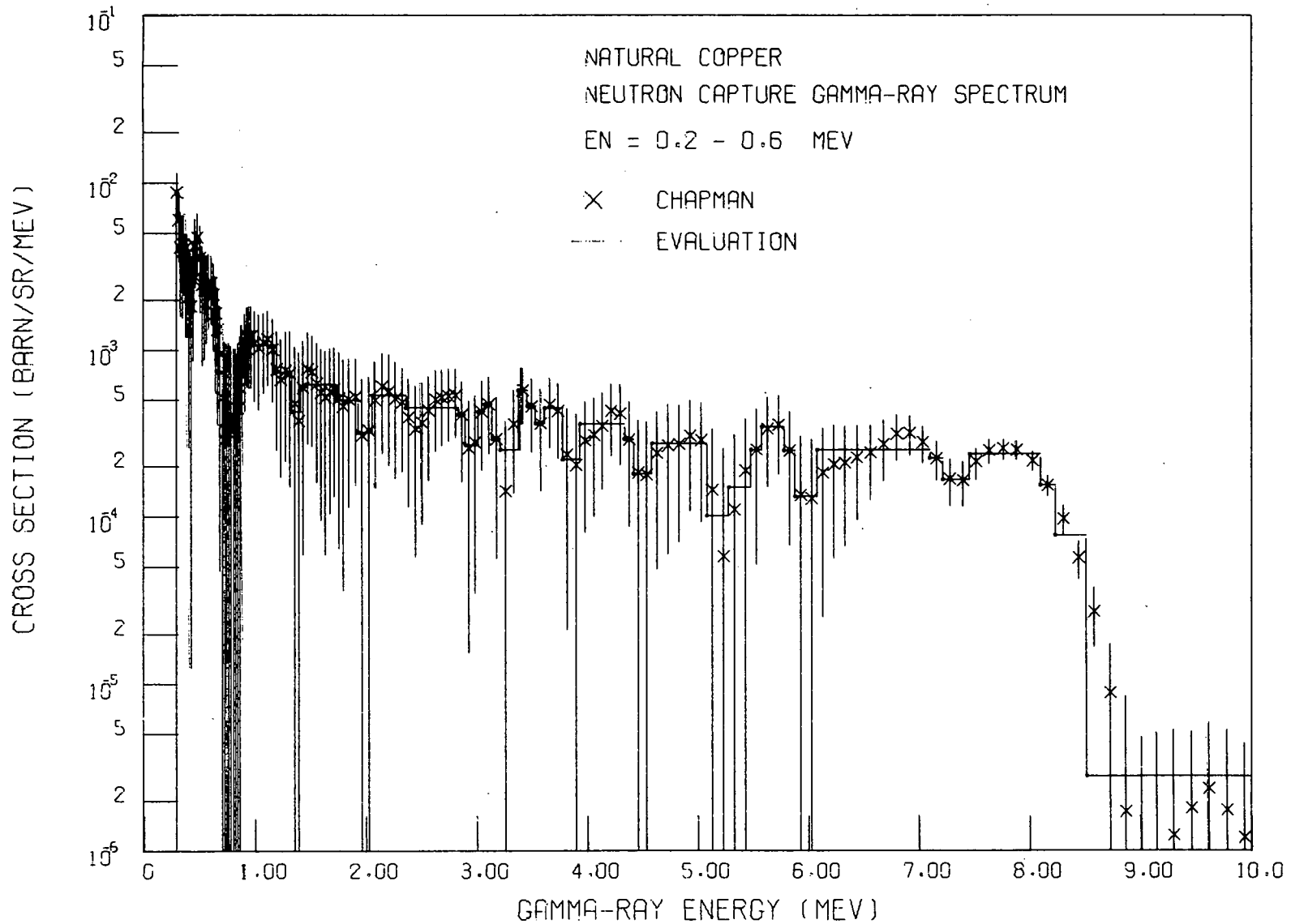
Fig. 28. Capture gamma-ray spectrum for Cu for E_n = 0.2 - 0.6 MeV.

23-458-79

43
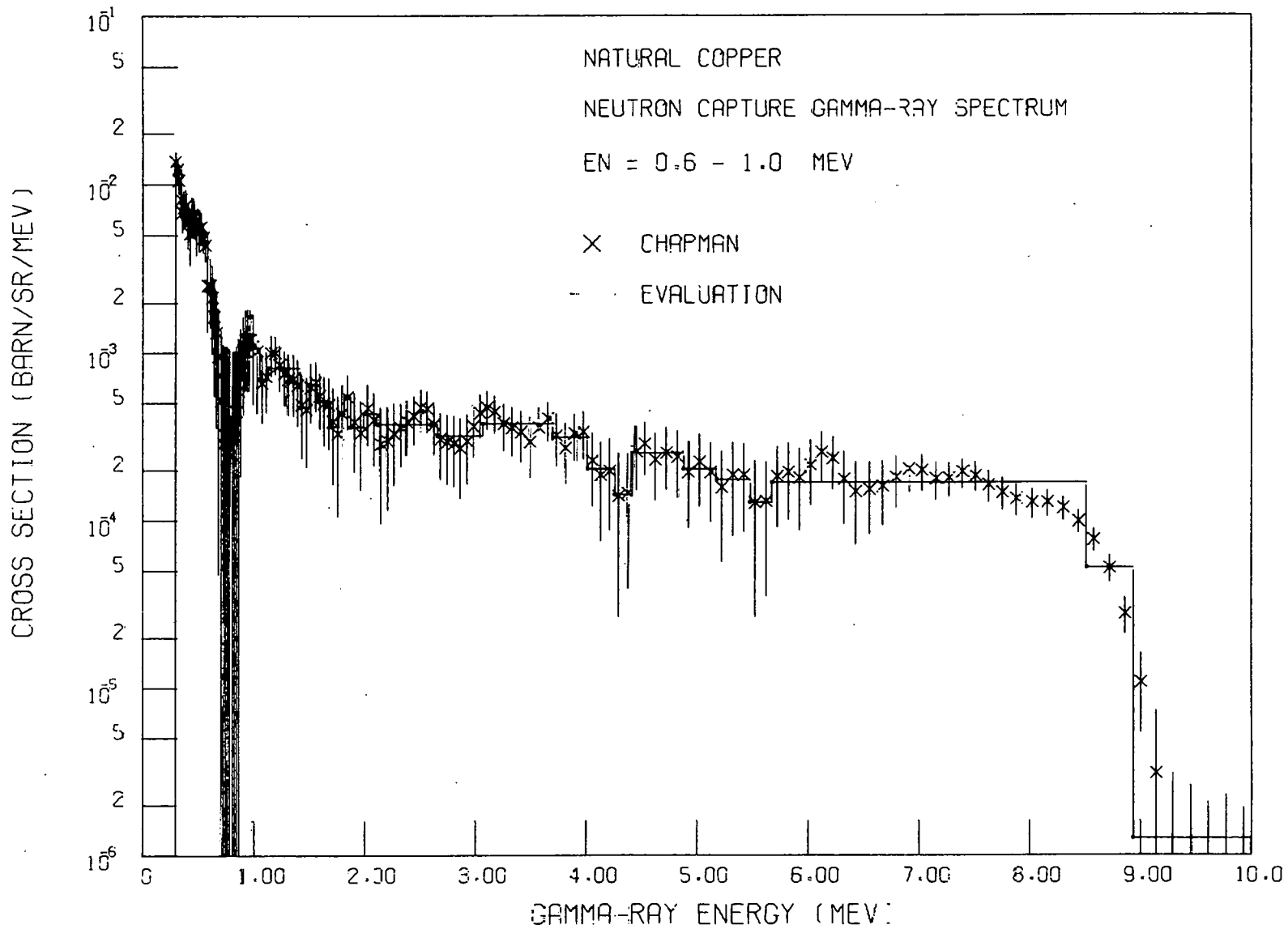
Fig. 29. Capture gamma-ray spectrum for Cu for E_n = 0.6 - 1.0 MeV. Contributions from gamma rays due to inelastic scattering were subtracted from the data.

6. UPDATES FOR LEAD (ENDF/B-V MAT 1382)

The ENDF/B-III evaluation and part of ENDF/B-IV have been described in detail.[10] The capture cross sections from 1 keV to 1 MeV were re-evaluated immediately after the ENDF/B-III evaluation was released. Structures in the total and elastic scattering cross sections were adjusted to be consistent with the new capture cross sections. This part of ENDF/B-IV was included in ref. 10. Another modification for ENDF/B-IV was the re-calculation of the neutron emission spectra to include precompound effects similar to the calculation for iron. A comparison of the calculated neutron emission spectrum for 14-MeV incident energy with available data has appeared in a critical review[43] of neutron emission spectra in ENDF/B-V for sodium, magnesium, aluminum, silicon, calcium, titanium, vanadium, chromium, iron, nickel, copper, niobium, tungsten, and lead. The ENDF/B-V emission spectra for iron and lead were found to be reasonably good. All others were either fair or poor.

Minor updates for ENDF/B-V are described below.

6.1 GAMMA-RAY PRODUCTION CROSS SECTIONS

The gamma-ray production cross sections for incident energies from 0.6 to 20 MeV measured by Chapman and Morgan[44] were adopted. Detailed comparisons of the data with the ENDF/B-IV values and with other available data are given in ref. 44. Since simultaneous analysis of neutron emission spectra and gamma-ray production spectra for each reaction was not performed, there may be inconsistencies in the evaluation, and, in particular, energy conservation may be violated.

6.2 (n,n'), (n,2n), AND (n,3n) CROSS SECTIONS

The (n,2n) cross sections from 7 to 15 MeV were revised according to the recent data of Frehaut and Mosinski.[45] There were no data available previously in this energy range. The extrapolation to 20 MeV was based on the ^{204}Pb data taken from BNL-325.[16] The (n,n') and the (n,3n) cross sections were revised accordingly to conserve the total reaction cross sections. Figure 30 compares these new values with ENDF/B-IV and the available data.

ORNL-DWG 82-9816

NATURAL LEAD
● (n, 2n) FREHAUT AND MOSINSKY
△ 204Pb (n, 2n) BNL- 325 (1976)
—— ENDF/B - V
- - - ENDF/B - IV
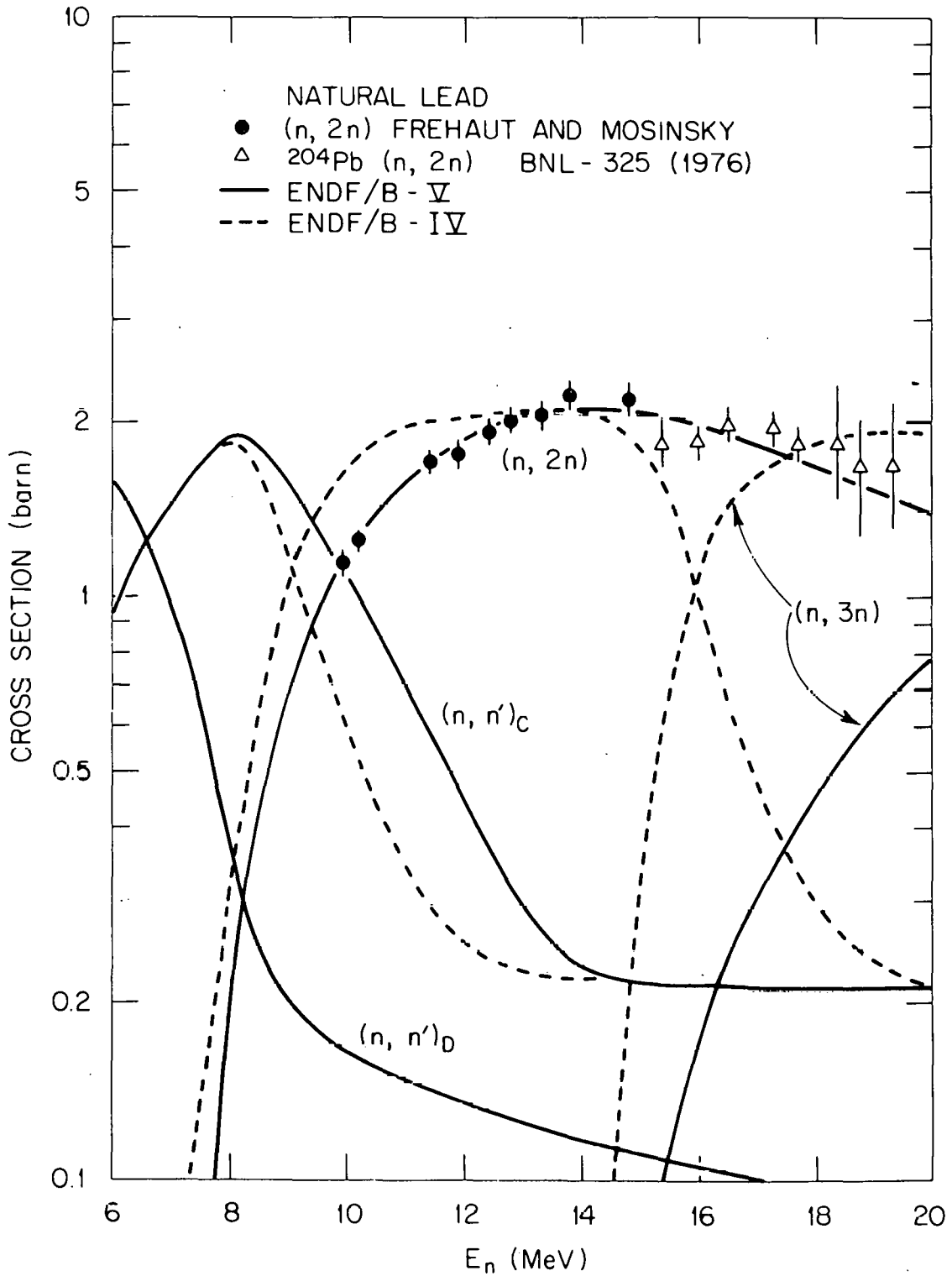
Fig. 30. The Pb(n,n'), (n,2n), and (n,3n) cross sections in ENDF/B-IV and -V and experimental data.

6.3 CAPTURE CROSS SECTIONS

From 3 to 20 MeV, several sets of capture cross sections are available for ^{208}Pb in BNL-325.[16] The only measured cross section for natural lead above 3 MeV is at 14.1 MeV by Cvelbar.[46] This value is in good agreement with the ^{208}Pb data. Therefore, the eye-guide curve drawn in BNL-325 through the available data of ^{208}Pb from 3 to 20 MeV for ENDF/B-V was taken.

6.4 COVARIANCE FILE

Covariance data were given for total, elastic scattering, non-elastic, inelastic, (n,2n), (n,3n), and capture cross sections. Derived sections (NC subsections) reflect how the cross-section files were generated.

In general, covariances were determined from $\pm 2\sigma$ error bands where data exist. The error bands were extended and enlarged to cover energy regions lacking experimental data. Long-range covariances reflect systematic errors common to all data sets. Medium-range covariances reflect differences in energy coverage by different data sets and differences in experimental techniques within the same data sets. Short-range covariances reflect meaningful structures in the cross sections and/or threshold effects. Statistical errors are nonexistent in the evaluated cross sections.

As in the case of iron,[5] absolute uncertainties were used, in addition to fractional uncertainties, to help keep the files short. The absolute components are the most useful for total cross-section minima and near thresholds.

Most cross sections for lead were evaluated with guidance from model calculations. However, for energy regions in which model calculations were used directly, uncertainty estimates were based on a general understanding of the adequacy or inadequacy of various models rather than on model parameter variations.

7. CONCLUSIONS AND RECOMMENDATIONS

Noted below are the areas where evaluations can be improved, where data are needed, where new data have become available, and where improved nuclear model codes can be put to good use.

Carbon. The existing information[11] for neutron emission spectra from $^{12}C(n,n'3\alpha)$ reaction remains poor, and no credible nuclear model is available to aid the evaluation. Also, neutron-energy distribution measurements for at least five angles are needed.

High-resolution total and differential elastic scattering cross sections for ^{13}C by Lane et al.[48] could be used to improve the existing evaluation up to 4.81 MeV, particularly the standard scattering cross sections below 2 MeV.

Calcium. The recent measurement[49] for the (n,p) cross sections suggests that our evaluation for these cross sections for E_n between 3 and 6 MeV should be lowered by about 30%. Since the (n,p) cross sections in this energy range are the largest of all reaction cross sections, a reduction as large as 30% should not be made without carefully studying its impact on other cross sections.

Iron. A recent study[50] of the radiative width of the 27.7-keV s-wave resonance in ^{56}Fe yields 1.01 eV as opposed to our evaluated value of 1.4 eV. The indicated reduction would not only reduce neutron capture in nuclear reactors and shields but also reduce the total cross section at the 24.3-keV minimum by about 20%.[51]

For 14-MeV incident neutron, the measured angular distributions[52,53] for outgoing neutrons between 4 and 10 MeV show a factor of two anisotropy (ratio of forward emission to 90-degree emission in the center-of-mass frame). These angular distributions have been reproduced with our improved version of the TNG code.[54] This model analysis could be used to generate complete angular spectra in evaluated form for incident neutron energies between 5 and 20 MeV.

High-quality data[34,36] for the proton and alpha-particle production cross sections at 14.8 MeV exist for iron but have not been used in the evaluation. The corresponding evaluated cross section for alpha-particle production is in good agreement with this new information, but the evaluated value for protons is 22% lower. A recent model analysis[9] reproduces these new data well but has not been generalized to include gamma-ray production.

Copper. As indicated, the total cross sections between 100 and 200 keV need to be refined. A recent, but not yet published, measurement by Harvey[55] should be examined.

Two measured spectra of gamma rays produced by thermal neutron capture are in a factor-of-two disagreement. One is by Orphan et al.[56] and the other by Maerker and Muckenthaler.[57] The former[56] was adopted in the evaluation and could be the wrong choice. These data should be examined more carefully, perhaps with the aid of nuclear model analysis.

The 14-MeV neutron emission spectrum in copper lacks a high-energy tail (the precompound component) as indicated by direct comparison[43] with available data and by analysis[58] of the leakage spectrum from a sphere pulsed with 14-MeV neutrons.

Energy imbalances in the copper evaluation could not be checked[25] because of the "elemental Q-value" problem but are known to exist.[59] The problem could be solved by performing isotopic evaluations for ^{63}Cu and ^{65}Cu.

Improved evaluations for the $^{63}Cu(n,\alpha)$ and the $^{63,65}Cu(n,2n)$ cross sections now exist[60] and should be adopted in the general-purpose file. The evaluations were based on the generalized least-squares techniques and made use of ratio data.

Lead. Energy imbalances in the lead evaluation are known to exist.[25] This is expected since several partial updates were made to the originally consistent evaluation.[10] Consistent model analysis for lead is time-consuming because calculations must be made for three isotopes. An update similar to that done for the iron evaluation may be advisable.

In conclusion, it should be noted that good evaluations eventually become obsolete, at least partially, as more accurate data become available and as more advanced nuclear model codes and evaluation tools are developed. In addition, improvements in computing facilities and transport codes, as well as new applications, invariably call for more details in the evaluated data.

REFERENCES

1. C. Y. Fu and F. G. Perey, *Atom. Data Nucl. Data Tables* , **22**, 249 (1978).

2. C. Y. Fu and F. G. Perey, "Neutron Scattering Cross Sections of Carbon below 2 MeV for ENDF/B-V," in *ENDF/B-V Cross Section Measurements Standards*, Ed(s). A. D. Carlson and M. R. Bhat, Brookhaven National Laboratory Report (in press).

3. C. Y. Fu, *Atom. Data Nucl. Data Tables* **17**, 127 (1976).

4. D. M. Hetrick and C. Y. Fu, *A Calculation of Neutron and Gamma-Ray Production Cross Sections for Calcium from 8 to 20 MeV*, ORNL/TM-7752, ENDF-308, Oak Ridge National Laboratory, Oak Ridge, Tenn., 1981.

5. C. Y. Fu and F. G. Perey, *Evaluation of Neutron and Gamma-Ray Production Cross Sections for Natural Iron (ENDF/B-V MAT 1326)*, ORNL/TM-7523, ENDF-302, Oak Ridge National Laboratory, Oak Ridge, Tenn., November 1980.

6. C. M. Perey and F. G. Perey, *Evaluation of Resonance Parameters for Neutron Interaction with Iron Isotopes for Energies up to 100 keV*, ORNL/TM-6405, ENDF-298, Oak Ridge National Laboratory, Oak Ridge, Tenn., Sepember 1980.

7. C. Y. Fu, "A Two-Step Hauser-Feshbach Model Code with Precompound Effects and Gamma-Ray Cascades," p. 328 in *Nuclear Cross Sections and Technology, Proc. Conf.*, Vol. I, National Bureau of Standards Special Publication SP-425, 1975.

8. J. E. White, C. Y. Fu, and K. J. Yost, *Nucl. Sci. Eng.*, **51**, 496 (1973).

9. C. Y. Fu, *A Consistent Nuclear Model for Compound and Precompound Reactions with Conservation of Angular Momentum*, ORNL/TM-7042, Oak Ridge National Laboratory, Oak Ridge, Tenn., May 1980.

10. C. Y. Fu and F. G. Perey, *Atom. Data Nucl. Data Tables*, **16**, 409 (1975).

11. J. Lachkar et al., *An Evaluation of the Neutron-Induced Scattering Reaction and Photon-Production Cross Sections of Carbon*, NEANDC(E) 168 "L", INDC (FR-7/L, 1975.

12. G. M. Frye, Jr., L. Rosen, and L. Stewart, *Phys. Rev.* **99**, 1375 (1955).

13. B. Antolkovic and Z. Dolenec, *Nucl. Phys.*, **A237**, 235 (1975).

14. B. Antolkovic and J. Hudomalj, *Nucl. Phys.*, **A237**, 253 (1975).

15. U. N. Singh, *Phys. Rev.*, **C10**, 2143 (1974).

16. D. I. Garber and R. R. Kinsey, *Neutron Cross Sections*, BNL-325, Third Edition, Vol. II, Brookhaven National Laboratory, Upton, N.Y., 1976.

17. B. J. Allen et al., "Neutron Capture Mechanism in Light and Closed Shell Nuclides," p. 360 in *Proc. Conf. Nucl. Cross Sections and Tech.*, NBS-SP-425, 1975.

18. A. R. De L. Musgrove et al., "Odd-Even Effects in Radiative Neutron Capture by Ca-42, Ca-43, Ca-44," *Nucl. Phys.* **A279**, 317 (1977).

19. F. Cvelbar, NIJS-R-505, Inst. Josef Stefan, Ljubljana, Yugoslavia, 1967.

20. M. Kawai, N. Yamano, and K. Koyama, "Request to Evaluating Neutron Cross Section of Structural Material for Shielding Application," p. 586 in *Proc. Conf. Nucl. Cross Sections for Tech.*, NBS-SP-594, 1979.

21. A. B. Smith, Argonne National Laboratory, personal communication to C. Y. Fu, Oak Ridge National Laboratory, Oak Ridge, Tenn., 1980.

22. C. M. Lederer and V. S. Shirley, *Table of Isotopes*, 7th Edition, 1978.

23. E. D. Arthur and P. G. Young, *Evaluated Neutron-Induced Cross Sections for $^{54,56}Fe$ to 40 MeV*, LA^8626-MS, ENDF-304, Los Alamos Scientific Laboratory, 1980.

24. A. Gilbert and A. G. W. Cameron, *Can. J. Phys.* **43**, 1446 (1965).

25. R. E. MacFarlane, "Energy Balance of ENDF/B-V," *Trans. Am. Nucl. Soc.* **33**, 681 (1979).

26. C. Y. Fu and F. G. Perey, "Summary Documentation for Iron (MAT 1192)," in *ENDF/B Summary Documentation* compiled by D. Garber, ENDF-201, 2nd edition, 1975.

27. V. J. Orphan, C. G. Hoot, and Joseph John, Gulf Radiation Technology Report RT-A10753, 1971; revision by V. C. Rogers, Intelcom Radiation Technology, personal communication, 1973.

28. J. K. Dickens, G. L. Morgan, and F. G. Perey, *Nucl. Sci. Eng.* **50**, 311 (1973).

29. G. T. Chapman, G. L. Morgan, and F. G. Perey, *A Re-Measurement of the Neutron-Induced Gamma-Ray Production Cross Sections for Iron in the Energy Range 850 keV < E_n < 20.0 MeV*, ORNL/TM-5416, Oak Ridge National Laboratory, Oak Ridge, Tenn., July 1976.

30. D. M. Drake, E. D. Arthur, and M. G. Silbert, *Nucl. Sci. Eng.* **65**, 49 (1978).

31. M. K. Drake and M. P. Fricke, "Evaluation of Neutron and Photon-Production Cross Sections for Natural Copper," DNA-3356F, Defense Nuclear Agency, 1974.

32. D. L. Allan, *Nucl. Phys.* **24**, 274 (1961).

33. R. S. Storey, *Proc. Phys. Soc.* **75**, 526 (1960).

34. S. M. Grimes, *Phys. Rev.* **C19**, 2127 (1979). R. C. Haight and S. M. Grimes, UCRL-80235, Lawrence Livermore Laboratory, 1977, and personal communication, 1977.

35. F. M. Mann and R. E. Schenter, "He Production - An Example of Hauser-Feshbach Calclations," in *Symp. on Neutron Cross Sections from 10 to 40 MeV*, BNL-NCS-50681, Brookhaven National Laboratory, 1977.

36. H. Farrar IV and D. W. Kneff, "Helium Generation In Twelve Pure Elements at 14.8 MeV," *Trans. Am. Nucl. Soc.* **28**, 197 (1978), and personal communication, 1977.

37. H. Alter, in *ENDF/B-IV Dosimetry Files*, ed. B. A. Magurno, BNL-NCS-50446, ENDF-216, Brookhaven National Laboratory, 1975.

38. F. G. Perey, Oak Ridge National Laboratory, personal communication with C. Y. Fu, Oak Ridge National Laboratory, 1976.

39. J. F. Whalen, CSISRS data tape (1970).

40. K. K. Seth, *Phys. Lett.*, **16**, 306 (1965).

41. J. Rainwater, *Bull. Am. Phys. Soc.*, **8**, 334 (1962).

42. G. T. Chapman, *The Cu(n,xγ) Reaction Cross Section for Incident Neutron Energies Between 0.2 and 20.0 MeV*, ORNL/TM-5215, Oak Ridge National Laboratory, Oak Ridge, Tenn., February 1976.

43. D. M. Hetrick, D. C. Larson, and C. Y. Fu, "Neutron Emission Spectra Induced by 14-MeV Neutrons from the Evaluated Nuclear Data File (ENDF/B-V) - A Critical Review," p. 765 in *Proc. Conf. on Nucl. Cross Sections for Tech.*, NBS-SP-594, 1979.

44. G. T. Chapman and G. L. Morgan, *The Pb(n,xγ)I Reaction for Incident Neutron Energies Between 0.6 and 20 MeV*, ORNL/TM-4822, Oak Ridge National Laboratory, Oak Ridge, Tenn., February 1975.

45. J. Frehaut and G. Mosinski, "Measurement of (n,2n) and (n,3n) Cross Sections at Incident Energies Between 8 and 5 MeV," *5th Int. Symp. on Interaction of Fast Neutrons with Nuclei*, Gaussig, DDR, 1975.

46. F. Cvelbar, *Nucl. Instr. Meth.* **44**, 292 (1966).

47. G. F. Auchampaugh, S. Plattard, and N. W. Hill, *Nucl. Sci. Eng.*, **69**, 30 (1979).

48. R. O. Lane et al., *Phys. Rev.* **C23**, 1883 (1981).

49. C. Murray Bartle, University of Cape Town, South Africa, personal communication, 1976.

50. K. Wisshak and F. Kappeler, *Nucl. Sci. Eng.* **77**, 58 (1981).

51. H. I. Liou, *Nucl. Sci. Eng.*, **70**, 150 (1979).

52. D. Hermsdorf, A. Meister, S. Sassonoff, D. Selliger, K. Seidel, and F. Shalin, *Differentielle Neutronenemissionsquerschnitte $\sigma_{nM}(E_0;E;0)$ bei 14.6 MeV Einschussenergie fue die Elemente Be, C, Na, Mg, Al, Si, P, S, Ca, Ti, V, Cr, Mn, Fe, Co, Ni, Cu, Zn, Ga, Se, Br, Zr, Nb, Cd, In, Sn, Sb, I, Ta, W, Au, Hg, Pb, und Bi*, ZKF-277(U), Zentralinstitut fur Kernforschung, 1975.

53. J. L. Kammerdiener, *Neutron Spectra Emitted by ^{239}Pu, ^{238}U, ^{238}U, Pb, Nb, Ni, Al, and C Irradiated by 14-MeV Neutrons*, UCRL-51232, University of California, 1972.

54. C. Y. Fu, "Development and Applications of Multi-Step Hauser-Feshbach Pre-equilibrium Model Theory," in *Nuclear Theory for Applications - 1980, Proc. Interregional Advanced Training Course on Applications of Nuclear Theory to Nuclear Data Calcuations for Reactor Design*, held at Trieste, Jan. 28—Feb. 22, 1980.

55. J. A. Harvey, Oak Ridge National Laboratory, personal communication with C. Y. Fu, Oak Ridge National Laboratory, 1981.

56. V. J. Orphan, C. G. Hoot, and Joseph John, GA-10248, General Atomics, 1970.

57. R. E. Maerker and F. J. Muckenthaler, ORNL-4382, Oak Ridge National Laboratory, Oak Ridge, Tenn., 1969.

58. R. J. Howerton, *Data Testing Results for the ENDF/B-V Evaluated Neutron Data File*, UCID-18731, Lawrence Livermore Laboratory, 1980.

59. C. Y. Fu, "Evaluation of Photon Production Data from Neutron Induced Reactions," p. 753 in *Proc. Conf. on Nucl. Data Evaluation Methods and Procedures, held at Brookhaven National Laboratory, Sept. 22-25, 1980*.

60. C. Y. Fu and D. M. Hetrick, "Experience in Using the Covariances of Some ENDF/B-V Dosimetry Cross Sections: Proposed Improvements and Additions of Cross-Reaction Covariances," Fourth ASTM-EURATM Symposium on Reactor Dosimetry, March 22-26, 1982, National Bureau of Standards, Gaithersburg, Maryland.

ORNL/TM-8283
ENDF-325
Dist. Category UC-79d

INTERNAL DISTRIBUTION

1-2. L. S. Abbott
3. Z. W. Bell
4. G. de Saussure
5. J. K. Dickens
6-8. EPIC
9. G. F. Flanagan
10-14. C. Y. Fu
15. J. A. Harvey
16. D. M. Hetrick
17. D. C. Larson
18-22. F. C. Maienschein
23. D. K. Olsen
24-28. R. W. Peelle
29. F. G. Perey
30. R. W. Roussin

31. C. R. Weisbin
32. L. W. Weston
33. A. Zucker
34. P. W. Dickson, Jr. (consultant)
35. H. J. C. Kouts (consultant)
36. W. B. Loewenstein (consultant)
37. Richard Wilson (consultant)
38-39. Laboratory Records
40. Laboratory Records-RC
41. ORNL Patent Office
42. Central Research Library
43. ORNL Y-12 Technical Library
    Document Reference Section

EXTERNAL DISTRIBUTION

44. Office of Assistant Manager for Energy Research and Development, Department of Energy, Oak Ridge Operations, Oak Ridge, TN 37830
45. M. R. Bhat, Building 197D, National Nuclear Data Center, Brookhaven National Laboratory, Upton, Long Island, NY 11973
46. Phillip B. Hemmig, Reactor Physics Branch, Division of Reactor Research and Technology, DOE, Washington, DC 20645
47. R. J. Howerton, L-71, Lawrence Livermore Laboratory, P. O. Box 808, Livermore, CA 94550
48. Odelli Ozer, Nuclear Safety and Analysis Department, Electric Power Research Institute, 3412 Hillview Avenue, P. O. Box 10412, Palo Alto, CA 94304
49. S. Pearlstein, Building 197D, National Nuclear Data Center, Brookhaven National Laboratory, Upton, Long Island, NY 11973
50. Robert Schenter, Hanford Engineering Development Laboratory, P. O. Box 1970, Richland, WA 99352
51. Stanley Whetstone, Division of Basic Energy Sciences, Department of Energy, Washington, DC 20545
52. P. G. Young, Los Alamos Scientific Laboratory, Los Alamos, NM 87545
53. S. Berk, Office of Fusion Energy, Department of Energy, Washington, DC 20545
54. E. T. Cheng, General Atomic Company, San Diego, CA
55-81. Technical Information Center, U. S. Department of Energy, Oak Ridge, TN 37830
82-171. Mary Rizzi, National Nuclear Data Center, ENDF, Brookhaven National Laboratory, Upton, Long Island, NY 11973
172-239. DNA Transport Distribution, Code AU
240-362. For distribution as shown in TID-4500 Distribution Category UC-79d, Liquid Metal Fast Breeder Reactor Physics - Base Technology.